EML 4905 Senior Design Project

A B.S. THESIS
PREPARED IN PARTIAL FULFILLMENT OF THE
REQUIREMENT FOR THE DEGREE OF
BACHELOR OF SCIENCE
IN
MECHANICAL ENGINEERING

INSPECTION VEHICLE FOR DEPARTMENT OF ENERGY HANFORD SITE UNDERGROUND CHANNELS

Jennifer Arniella
Daniel Giraldo
Gabriela Vazquez

Faculty Advisor: Dr. Benjamin Boesl

November 24, 2014

This B.S. thesis is written in partial fulfillment of the requirements in EML 4905. The contents represent the opinion of the authors and not the Department of Mechanical and Materials Engineering.

Ethics Statement and Signatures

The work submitted in this B.S. thesis is solely prepared by a team consisting of JENNIFER ARNIELLA, DANIEL GIRALDO, and GABRIELA VAZQUEZ and it is original. Excerpts from others' work have been clearly identified, their work acknowledged within the text and listed in the list of references. All of the engineering drawings, computer programs, formulations, design work, prototype development and testing reported in this document are also original and prepared by the same team of students.

Gabriela Vazquez	Jennifer Arniella	Daniel Giraldo
Team Leader	Team Member	Team Member

_____

Dr. Benjamin Boesl
Faculty Advisor

Table of Contents

List of Tables

List of Figures

List of Equations

Abstract

Breaking Under Ground (BUG) is a student-driven senior design group that has built a miniature inspection vehicle that travels through the United States Department of Energy Hanford Site underground tanks' refractory pad cooling channels. The vehicle consists of a small frame that houses four gearmotors each connected to a wheel. A magnetic plate sits on top of the vehicle so that the device runs upside down along the bottom of the tank to avoid existing debris and potentially damaging the refractory pad in which it travels through. A lead acid battery directly powers the four motors while an Arduino is used to regulate the voltage output. The vehicle also has a miniature camera to allow live visual feedback to site engineers.

The first retrieval of radioactive material at the Hanford Site began in 1944. This process recovered radioactive material from spent fuel and produced vast quantities of high level waste. There are twenty-eight double-shell tanks arranged in six underground tank farms each holding close to one million gallons of high-level waste; the AY tanks are the oldest of these double shell tanks at the site. In August of 2012, it was determined that waste had leaked into the annulus between the primary and secondary walls of AY-102 tank. It is believed that the high level radioactive waste leaked from the tank bottom flowed through the cooling channels of the refractory pad to the annulus.

Site engineers will use the inspection vehicle and live video feedback provided by the camera to gain further knowledge of the condition of the primary tank and source of leakage or potential crack. This design project is sponsored by the Department of Energy Environmental Management Office and the Applied Research Center's DOE-FIU Science and Technology Workforce Development Program.

1. Introduction

1.1. Problem Statement

The first retrieval of radioactive material at the United States Department of Energy (USDOE) Hanford Site began in 1944. This process recovered radioactive material from spent fuel and produced vast quantities of high-level waste. There are twenty eight double-shell tanks arranged in six underground tank farms each holding close to one million gallons of high level waste. [1] Each one consists of a primary tank and a secondary liner tank. As seen in Figure 1, the insulating refractory pad that rests on the secondary liner supports the primary steel tank; an annular space of 76.2 cm. is formed between the primary tank and secondary liner. Figure 2 shows a photo taken within the annulus of the double shell tank prior to any leakage during its initial installation. [2]

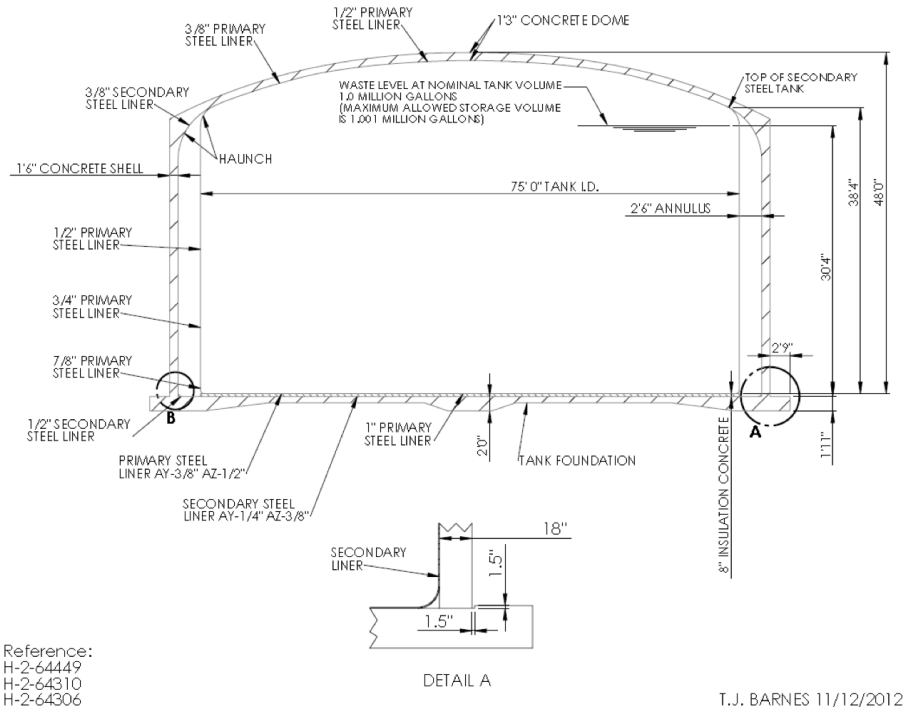

Figure 1. Double Shell Tank Cross Section

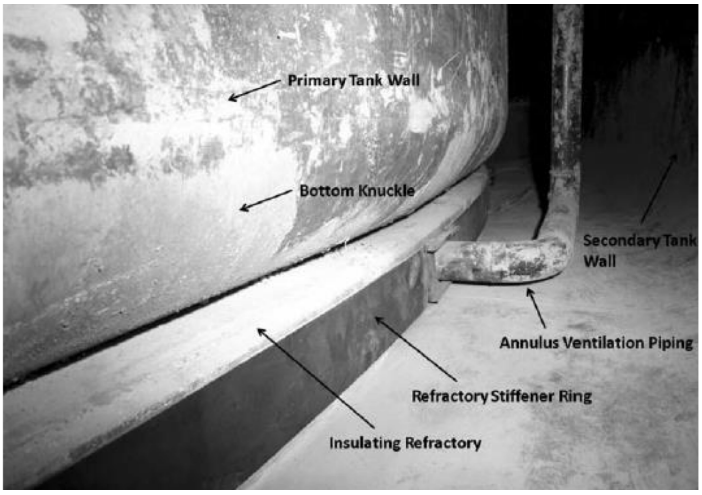

Figure 2. Annulus Detail

As mentioned previously, the primary tank rests on the refractory pad. Air distribution slots are cast into the top surface of the pad. Air supplied to the central air distribution chamber cools the primary tanks as it is drawn through the slots and exhausted from the annulus. The slot pattern and slot cross section vary by tank farm. The slot distribution seen in Figure 3 is the

pattern most generally used. The slots emanate in a radial pattern from two concentric air distribution circles surrounding the central air distribution chamber. The slot cross sections are extremely small as seen in Figure 4 and vary from 3.8 cm by 3.8 cm to a 6.35 cm by 3.8 cm and finally 7.62 cm by 3.8 cm. [3]

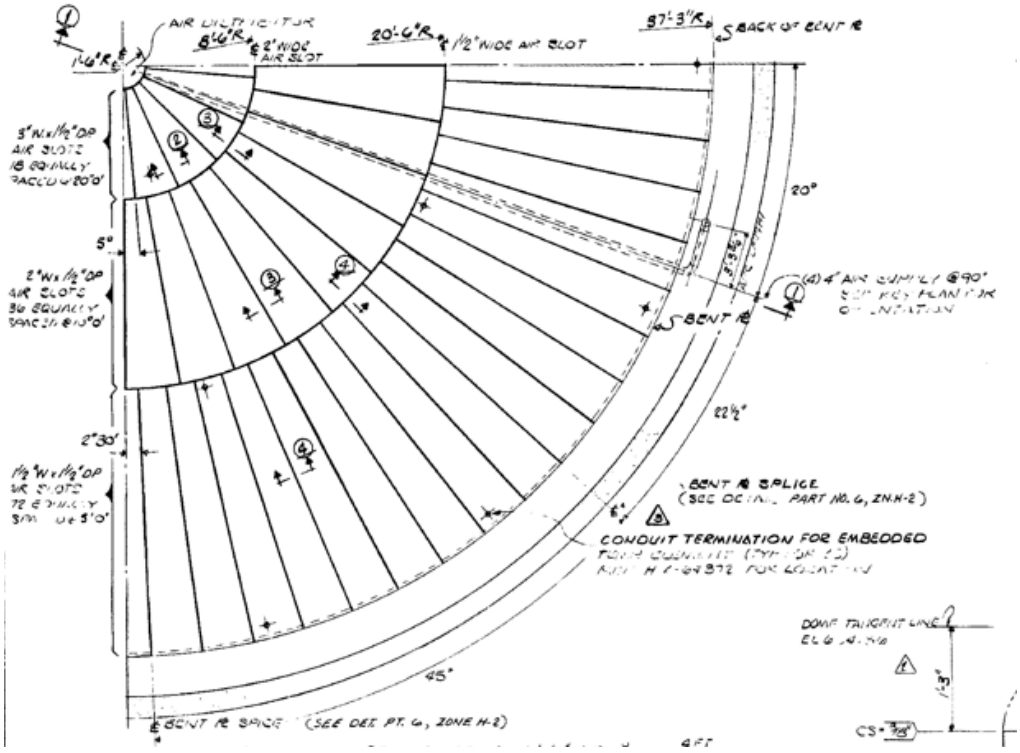

Figure 3. Air Distribution Slot Pattern

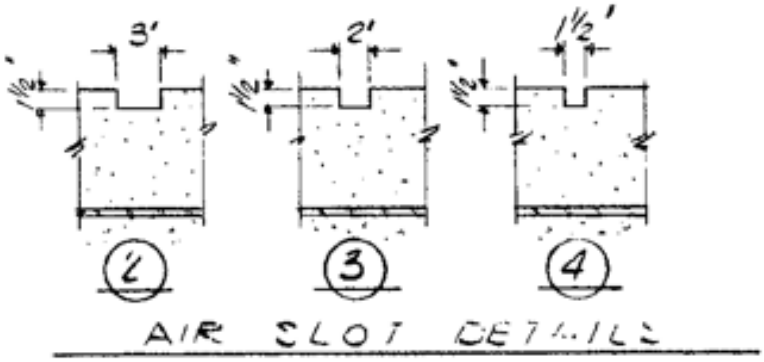

Figure 4. Square Slot Cross Section

The AY tanks are the oldest type of double shell tanks and the AY-102 tank was the first double-shell radioactive waste storage tank constructed at Hanford. The use life of the tanks was approximately 40 years and the tanks are currently at 45 years of use. In August of 2012, an accumulation of material was discovered at two locations on the floor of the annulus that separates the primary tank from the secondary liner tank as seen in Figure 5. The origin is believed to be a break in the bottom of the primary tank. This material has since been removed partially through evaporation as well as physical removal. [4][5]

Figure 5. High Level Waste on Annulus Floor

Hanford site engineers require a means to perform visual inspections of the primary tank bottom. The insulating refractory pad has a low shear strength and thus extremely friable. Previous attempts of inspection using a crawler were abandoned shortly after deployment due to the damage of the refractory pad created by the crawler's movement. A small remote camera was also attempted as a means of inspection but due to the rapid jerks of forward and backward motion it was difficult to record the distance within the channel.

The device required by site engineers should be capable of traveling within the refractory pad cooling channels while minimizing the contact to the refractory pad to avoid creating debris. The travel location needs to be recorded so that potential leaks or cracks can be identified for future repair and finally a high definition video signal is required for recording data. The device will also encounter harsh conditions and thus must be leak tight, corrosion resistant, radiation hardened and withstand a maximum operating temperature of 125 °F.

Breaking Under Ground (BUG) is a student-driven senior design group that has built a miniature inspection vehicle that is capable of travelling through the underground tanks' refractory pad channels. The vehicle consists of a small frame that houses four nano gearmotors each connected to a wheel. A magnetic plate sits on top of the vehicle so that the device runs upside down along the bottom of the tank to avoid existing debris and potentially damaging the refractory pad in which it travels through. A lead acid battery directly powers the four motors while an Arduino is used to regulate the voltage output. The vehicle also has a miniature camera to allow live visual feedback to site engineers.

1.2. Motivation

Leakage of the radioactive material into the subsurface soil is of a major concern and so the environmental impact is the foremost motivation. The largest waterway in the Pacific Northwest, the Columbia River is five miles from the Hanford site where the tanks are located. [6] It is extremely important to avoid contamination of such a major body of water that can affect not only its ecosystem but also the communities downstream that use that water as a source. Currently there is no leakage from the secondary tank but before waste continues to build up in the annulus and potentially deplete the reliability of the secondary liner it is important to identify the leakage source for repair. [5][7] An inspection tool is thus required to travel through the

refractory cooling channels as seen in Figure 6 to provide video feedback to site engineers of the primary tank conditions. [8]

Figure 6. Refractory Pad Cooling Channel (Air Slot)

A secondary motivation is the challenge the task presents. Site engineers originally contracted four different vendors to propose technologies but due to different limitations none of the proposed technologies are in current use. [9] The tool must have a failsafe tether in case of malfunction, thus an already minute device must be able to carry its own weight as well as drag the tether. The refractory pad has low shear strength and so the device must also avoid damaging the refractory pad as it travels through the first 4.87 m of the channel. [10] All in all, the major challenges of the task include the small size of the channels, the long distance that the tool must travel, the friable refractory pad, the high temperatures the tool must withstand, and the potentially radioactive conditions it may come into contact with.

1.3. Literature Survey

There are few robots specifically designed to be able to handle harsh conditions such as chemical disasters, much less on a micro scale. Not until the 2011 disaster of Fukushima did people start paying serious attention to the development of robots to be able to handle such conditions. According to an article published by the bulletin of the atomic scientist, “Robot to the

Rescue," DARPA launched a robotics challenge to start producing robots capable of operating in dangerous, degraded environments. [11]

This brought about the development of robots that slither according to Science news. Howie Choset is a roboticist who used the snake as reference to build a robot that can slither, roll, swim, and climb as seen in Figure 7. The robot has been successful as an inspection tool and is being tested to do search and rescue. The biggest problem that has been raised with the development of our robot is its ability to be able to make turns as sharp as 90 degrees however the research done by roboticist Howie Choset and biologist Robert Full show that by mimicking the anatomy of versatile animals this can be achieved. [12] [13]

Figure 7. Slither Robot

An article published by Edge of Technology uses as inspiration the agama lizard that can stick to walls and walk upside down giving us the vision for the vehicle to run upside down along the tank wall to avoid creating debris while running on the refractory pad. [11]

Research by MIT has developed magnets for robots that allow them to anchor themselves to pipe or ship hulls, they originally created this to assist underwater robots when they have to grip onto something when they need to turn, however it can be implemented on our design because it requires very little electrical energy to get the magnets activated. [14]

1.4. Survey of Related Standards

This design project is focused on the development of the first prototype of the inspection vehicle. Recommendations will be provided for materials and manufacturing if a second prototype are to be built for future deployment at the Hanford Site. For this process a set of standards must be adhered to in order to provide a safe, reliable and quality product.

As engineers safety is the top priority and with the conditions as mentioned to be encountered underground it is important to keep the public, workers, and the environment safe from the harmful effects of radiation. A guiding standard for this process would be the USDOE's technical standard: DOE-STD-1189-2008 Integration of Safety into the Design Process. The Standard provides guidance on the implementation of safety in design. [15]

Additionally, a particular material is required in order for the vehicle to operate in such harsh conditions. The American Society for Testing and Materials (ASTM) develops and publishes technical standards for specific materials. In this case, ASTM standards were used to find a material that can withstand the harsh conditions, specifically A666 Standard Specification for Annealed or Cold-Worked Austenitic Stainless Steel Sheet, Strip, Plate, and Flat Bar and ASTM A240 Standard Specification for Chromium and Chromium-Nickel Stainless Steel Plate, Sheet, and Strip for Pressure Vessels and for General Applications. [16]

Moreover, there are several components of the mechanical system of the vehicle. The International Organization for Standardization (ISO) provides the guidelines and specifications to ensure that the products and processes used are fit for their purpose. Using ISO 1000 International System of Units, the 2D mechanical drawings clearly communicate how the design is to be manufactured. And IS0 9000 Quality Management Systems certify a reliable motor production infrastructure. [17]

Finally, the Institute of Electrical and Electronics Engineers (IEEE) standards will be used to select the electrical components and to develop and operate the electrical system required to power the vehicle. [18]

1.5. Industry Design Alternatives

The first proposed alternative was presented by AREVA. AREVA prides itself in its expertise in engineering solution for double shell tank inspections, its knowledge and experience of the double shell tank environment and the understanding of constraints particular to the AY-102 inspection. After consulting with robotic and inspection experts in France to utilize global experience, AREVA proposed a rigid SeeSnake MicroReel as seen in Figure 8. The Seesnake is a semi-rigid video probe that allows for quick inspection and the ability to push past debris. The crawler is used to position the probe and the pusher mounted on the crawler is to push the probe into the slots. The cons associated with the proposed design is that it requires manual or mechanical assist from the surface, the push probe is not proven to navigate through a number of bends and there is no articulation on the camera. The total cost was approximately $1,000,000: $260,000 for materials cost and $730,000 labor costs.

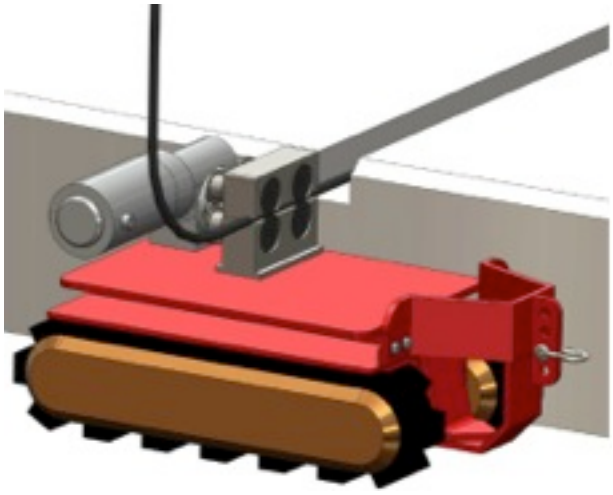

Figure 8. SeeSnake MircroReel

AREVA had a very high confidence level that the push probe would be able to navigate through the first 5.18 m of the refractory pad but had a moderate confidence level that the push probe would be able to navigate through the first elbow and continue through the second and third sections of the refractory pad. The board chose not to continue with this design. [9][19]

The second proposed design is a similar concept to the previously mentioned but presented by Vista Engineering Technologies is a crawler-mounted rolatube with a camera as seen in Figure 9. The rolatube has functioned for previous nuclear inspections and includes a repair capability with resin application, which is one of the benefits of the design. The downfall of the design presented is the crawler has yet to be designed. The crawler design is expected to be compact with a self-contained drive and axle with a tipping plow that ensures the crawler will land on its feet when sent down the annulus riser into the annulus.

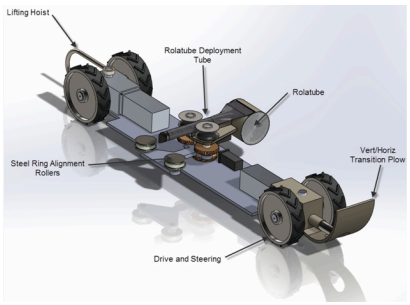

Figure 9. Rolatube Mounted on Crawler

The details of the rolatube as seen in Figure 10 demonstrates how the rolatube works. The rolatube extends through a friction drive as the magnetic guides position it. The rolatube also allows for a back drive if recovery is required in case of failure unit. The camera seen in Figure 11 is a small radiation tolerant camera with a light. The camera comes with a rotating special split viewing mirror too see the walls and middle slot exit. [9][20]

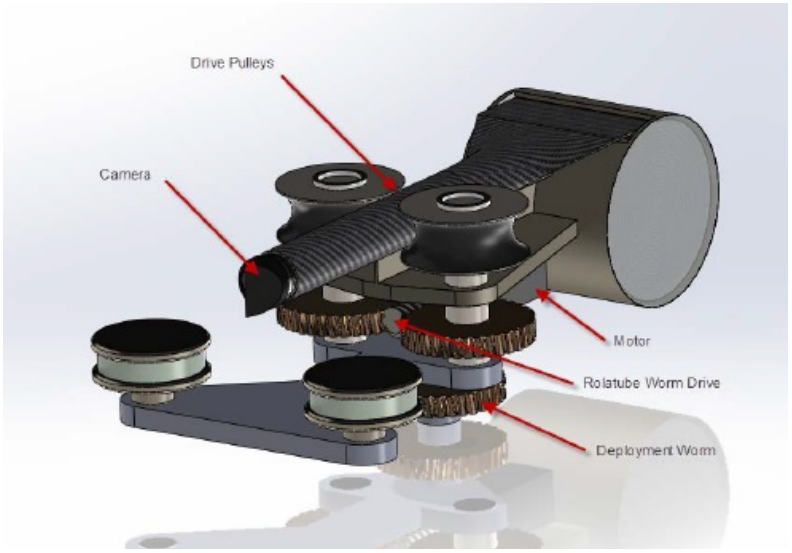

Figure 10. Detail of Rolatube

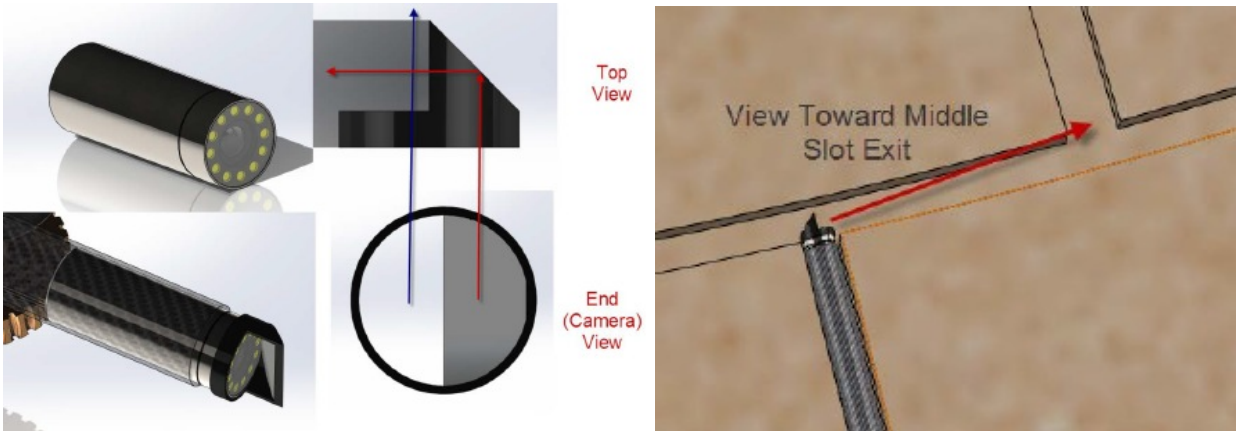

Figure 11. Rolatube Camera

IHI Southwest Technologies proposed a small remote camera that had been used to inspect a portion of the slots in some tanks. It was expected to be a four-wheeled micro robot with a separate delivery crawler that would deliver the inspection robot into the annulus. The cons of the tool was there was not a set device to deliver the inspection tool but the pros outweighed this factor in that IHI had prior nuclear experience, they delivered a competitive cost and schedule and the device had prior use underwater so the inspection tool was promising.

This device was the only device selected by the board for use. Once deployed, the photos revealed spalling on the slot walls, and accumulated debris on the floors as seen in Figure 12. The camera was not equipped to record travel distance; and its forward and backward motion were limited to rapid jerks making its actual location in the slot uncertain and the video trace of marginal value. The total cost was estimated at $75,300: $41,600 for the controller, $17,300 for the refractory air slots robot and then an additional $16,400 for the pan/tilt camera. The robot design, manufacture, mockups, testing, and administrative duties such as design documentation; onsite training and final reports were all taken into account for the price of each component. [9][21]

Figure 12. Debris inside Refractory Slot

2. Project Formulation

2.1. Project Objectives

For this research and design task, our objective is to effectively create a miniature inspection vehicle that can travel the first straight-line 4.87 m of the channel for each of the seventy two entry points, provide live visual feedback to site engineers via camera, and minimize damage to the refractory pad by using a magnet to hold the vehicle upside down on the tank bottom.

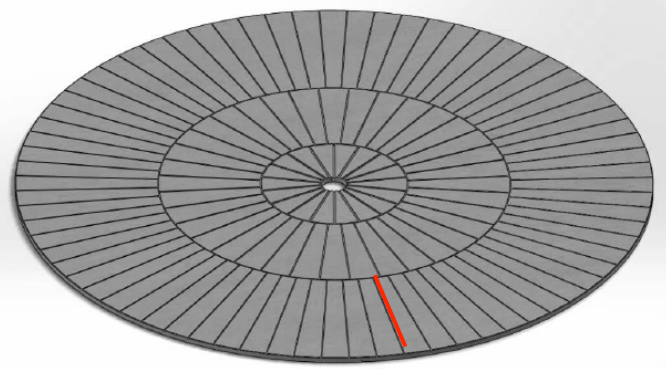

Figure 13. Travel Path

If the inspection device is able to successfully navigate thus far it will have already covered 45% of the total travel distance, providing Hanford Site engineers with an initial comprehension of channel conditions.

As a senior design group, this task is providing us the perfect opportunity to work as a team to solve a real world application challenge. This task not only requires the application of our technical skills but also functions as a professional development opportunity. It is our goal to work as a cohesive unit and responsible members of the team by meeting deadlines and completing original work. As engineers we are to act professionally and as faithful trustees, it our goal to respect the intellectual property of others thus throughout the design process and

compilation of this report we ensured to complete our own work and reference any resources that were used. It is also our ethical responsibility to complete jobs in the areas of our competence so team responsibilities were delegated based on each individual's strengths. Our aim is for every member to be in constant communication with others to ensure timely completion of the design and report.

Finally, it is our responsibility as future engineers to hold paramount the safety, health and welfare of the public in the performance of our professional duties. BUG's ultimate objective is to consider the environmental implications of high level waste leakage into the subsurface soil and fully comprehend the importance of our inspection device to function as a preventive measure to find and repair leaks so that they can be repaired to keep our environment and communities safe.

2.2. Design Specifications and Constraints

The tool is to provide a means for Hanford engineers to inspect the primary tank bottom of AY-102 by navigating the device through the refractory pad air slots. Specific requirements for the design include:

1. Navigate through 3.81 cm by 3.81 cm channel up to 4.87 m
2. Minimize damage to the refractory pad
3. Provide visual feedback of the tank bottom and refractory slots
4. In the event of a malfunction of the inspection tool, it should have a means for removal
5. Capable of exposure to elevated temperature and radiation levels (76.6 ºC, 85 Rad/hr)

BUG's final prototype expects to meet the listed challenges by creating a device with four motors and wheels allow it to travel like a vehicle through the channel. To minimize

damage to the refractory pad, a magnetic plate will is attached to the top of the vehicle so that the magnetic force holds the vehicle upside down along the tank bottom. The magnet is set a small distance away from the tank so that the magnetic force is strong enough to hold the vehicle up but does not add an additional frictional force to overcome. The vehicle also incorporates a camera to allow a visual of the tank bottom and refractory pad. Finally, the cables to each motor and the camera's line jacketed together function as a tether in case of device failure to pull the vehicle back out. Due to funding limitations, the final design specification of meeting temperature and radiation hardened criteria were not incorporated in the prototype but recommendations are provided for future prototype generations. These recommendations include but are not limited to the material 316 stainless steel will be used to manufacture the frame as it provides corrosion resistance and heat resistance up to 871°C as well as radiation tolerant.

3. Design Alternatives

The initial design consisted of a small tank type body that housed a camera and motors, whose body was connected to “tank tread” wheels. To avoid existing debris in the air slots and potentially damaging the refractory pad, the design has a magnetic tank tread so that it can run upside down along the bottom of the carbon steel tank.

Through discussion with Washington River Protection Solution engineers, an important aspect of the inspection tool is the live video stream so that distance traveled can be easily correlated with the video, and any obstructions at those distances can be repaired. It was also concluded that a tether was needed for the inspection tool as a full proof method to retrieve the tool in the event of malfunction. For this inspection tool, the tether was expected to consist of a camera fiber optic line and a control/power feed for steering and navigation. Figure 14 shows a 3D rendering of the initially proposed inspection tool as it would have been oriented upside down along the tank bottom.

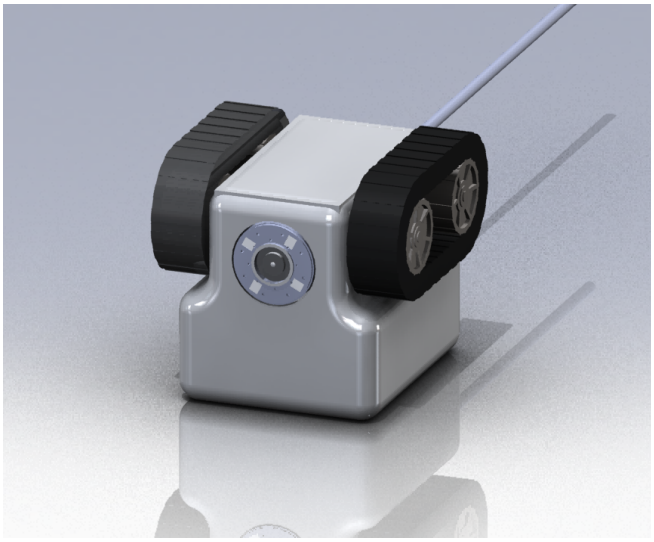

Figure 14. Rendering of Proposed Design

Figure 15 shows additional views with the internal components exposed. The components were sized using information from commercially available products. The body for the initially proposed tool is 3.04 cm by 3.04 cm by 2.92 cm. Motors contained in the body are attached to one wheel on each side and drive the opposite wheels via a track. Gears were also included to increase the torque from the motors that need to overcome the magnetic force and drag from the tether. [22]

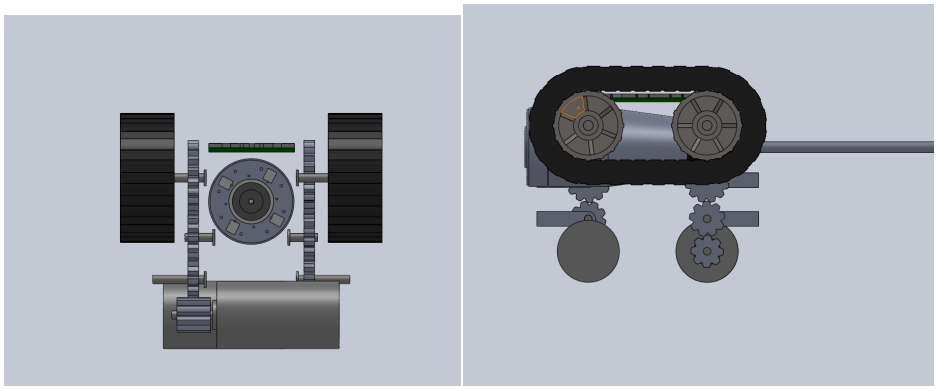

Figure 15. Front and Side View of Internal Components

In the prototype assembly of this design, many challenges were encountered. Initially, finding off the shelf available tank tread wheels of such small size was not possible and so an attempt was made to rapidly prototype wheels and use a rubber band as a tank tread but this was not feasible as seen in Figure 16.

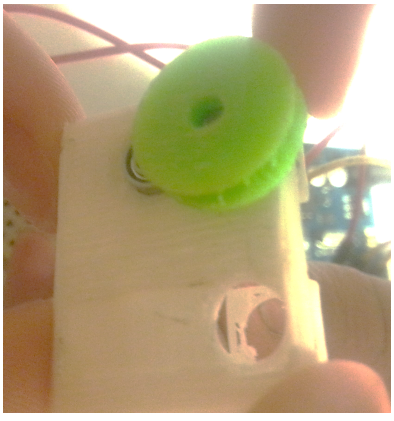

Figure 16. Printed Wheel

Then due to the limited space within the frame it was extremely difficult to set the gears within the supports as well as to align and merge precisely. This translated to the performance of the motor because the motor could not supply enough torque to rotate any of the gears due to all the interference created as seen in Figure 17.

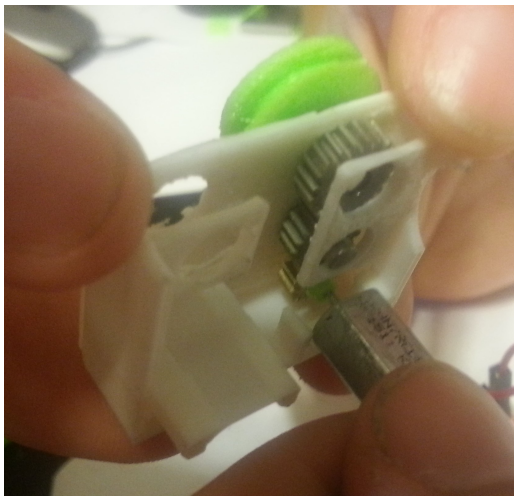

Figure 17. Prototype Assembly of Initial Design

4. Final Prototype

4.1. Design

Based on the lessons learned from our initial design and prototype, the final design is composed of four motors giving power to four wheels contained within a frame. It then has a magnet on top of the frame in order to hold the device upside down and travel through the slots without touching the refractory pad. This design was similar to our initial device but instead it contains two extra motors and the gears were eliminated to diminish the inefficiencies of the mechanism. Moreover, the wheels are offset in order to fit the motor in the width direction to connect directly to the wheels. The device was 2.54 cm in width and 1.52 cm in height.

The camera is positioned at the bottom of the device. Figure 18 shows the initial prototype of the final design. Moreover, it was observed that the cables powering the motor decreased the amount of force for the vehicle to move forward. Therefore, different ways were investigated to eliminate or downsize the cable size to decrease the required pulling force.

Figure 18. First Prototype of Final Design

In Figure 19, the position of the device inside the slot is shown using a wood channel with a piece of carbon steel on top as would be the refractory pad channel with a carbon steel tank above. The carbon steel attracts the magnet and holds it above the refractory pad to avoid creating debris.

Figure 19. Prototype within 3.81 cm by 3.81 cm Channel

In Figure 20, an image taken from the vehicle camera looking into the slot length is shown. Attaching a camera to the bottom of this device, allows the vehicle to function as an inspection tool to obtain pictures of a pathway without destroying the surrounding.

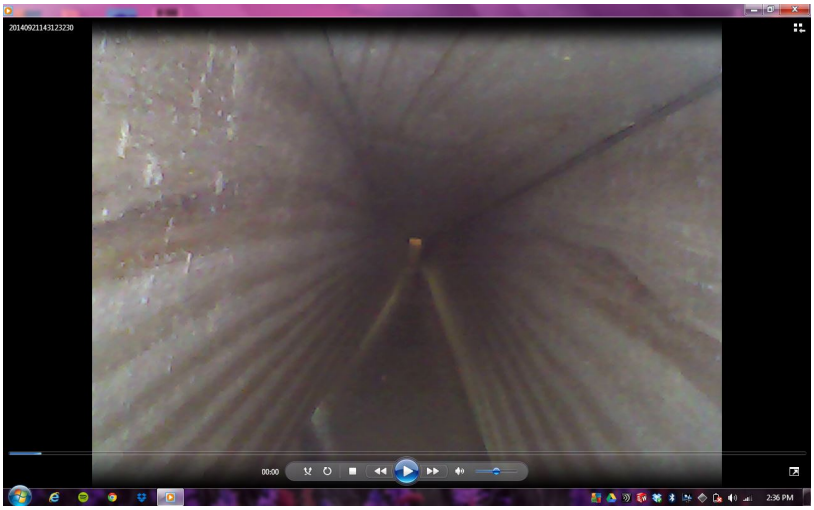

Figure 20. Camera View within the Channel

From our initial prototype of the final design we determined that for the design to potentially succeed, the individual components of the device had to be improved. For the second prototype, the motors, wheels, magnet, and the electronic controller were all improved. The previous motors used supplied a 0.098 mN-m maximum torque while the new motors are

capable of 21.15 mN-m. To accommodate for the change in motor and its shaft, thicker rubber wheels were found whose borehole matched the diameter of the shaft. Finally, to accommodate for the smaller diameter of the wheels a thinner magnet had to be used to allow the wheels to have contact with the tank bottom. The device is now 3.09 cm wide by 3.68 cm in length and 2.05 cm in height, giving it ample space to travel through the 3.81 cm by 3.81 cm channel. Figure 21 demonstrates a Solidworks rendering of the updated design.

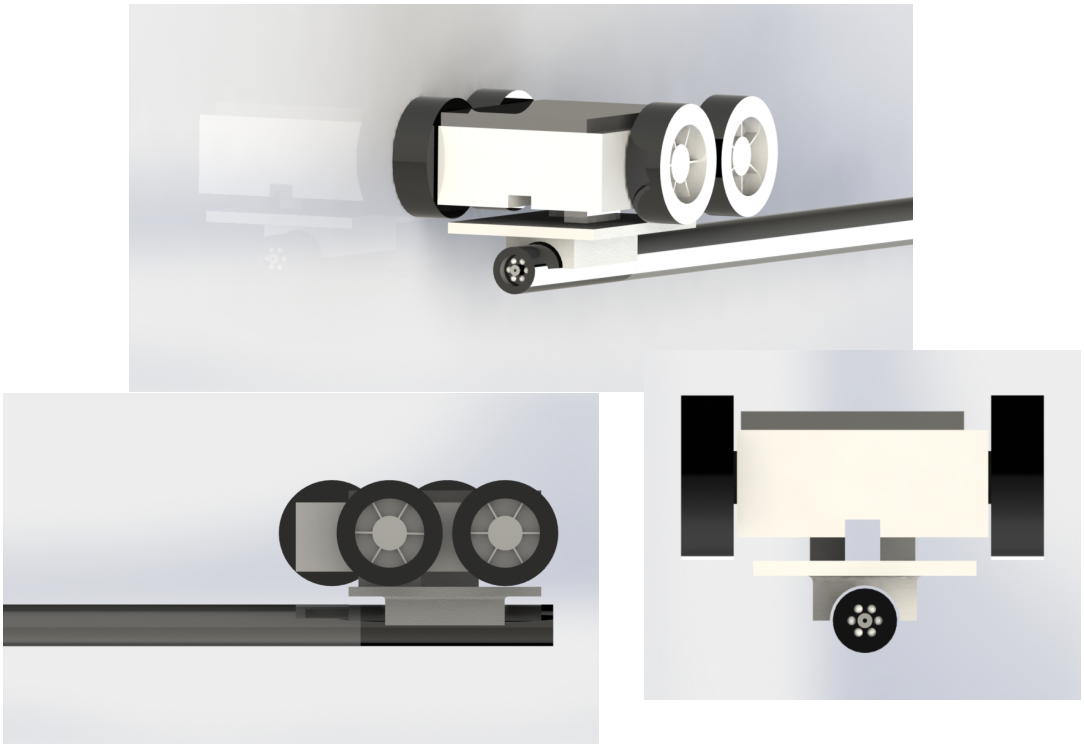

Figure 21. Rendering of Second Prototype of Final Design

As seen in the Figure 22, the device frame was printed using a rapid prototyping 3D printer and held together using super glue. The camera was also attached using super glue. In the future, the frame will be machined using stainless steel and the camera will have an encapsulating piece to hold it in place.

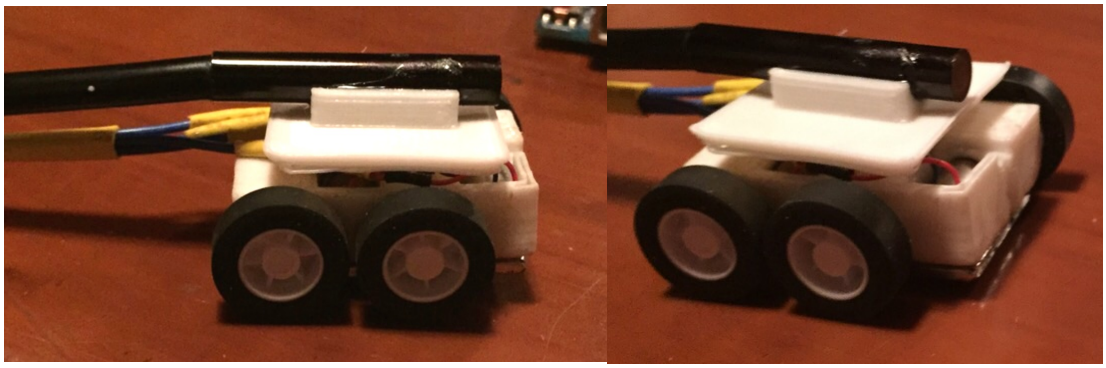

Figure 22. Second Prototype of Final Design

4.2. Major Mechanical Components

The components that will be used in the inspection device are listed in

Table 1. Determining the frame dimensions is an essential part of this project since our frame needs to accommodate multiple components in a small space, while at the same time, allowing the components to interact well with each other. The magnetic plate needs to be strong enough to attach the inspection device to the carbon steel tank while at the same time meet the available space between the inspection device and tank. The motors were carefully selected in order to fit in the constrained dimensions while providing enough power and torque for the wheels.

Table 1. Components list with main specifications and manufacturer

Component	Specifications	Manufacturer	Photo
Magnet Plate	Dimensions: 2.54-cm by 1.905-cm by 0.1587-cm Material: NdFeB, Grade N42 Weight: 2.032 oz Max Pull Force: 104.96 oz Max Operating Temp: 80ºC Part Number: BX0C1	KJ Magnetics	
Sub-Micro Plastic Planetary Gear Motor	Diameter: 0.599-cm Body Length: 2.189-cm Torque: Starting 21.15 mN-m Weight: 0.096 oz Gear Ratio: 136:1 Material: Nylon Shaft, Liquid Crystal Polymer gears Plating/Coating: Nickel	Pololu	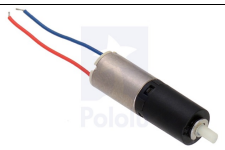
Wheels	Diameter: 0.889-cm Bore Diameter: 0.1008-cm Face Width: 0.635-cm Material: Acrylonitrile Butadiene Styrene with natural rubber tires	Pololu	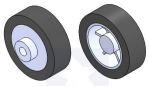
Power Line	Wire Gauge: 30 AWG Outer Diameter: 0.1092-cm	Pololu	
Frame (Body)	Material: ABS Filament Width: 3.09-cm Length: 3.683-cm Height: 2.054-cm	3-D Printer	
Camera	Dimensions: 499.87-cm x 0.5334-cm diameter. Camera and Cable Weight: 7 oz Resolution: 640 x 480 Built in LED lights: 6 LED Image Format: VGA/QVGA USB Interface: USB 2.0 Waterproof	EggsNow	

4.3. Recommendations

When manufacturing the actual device for the deployment at the site the following recommendations should be considered:

1. Frame and camera holder should be manufactured with 316 stainless steel. According to ASTM A240 and ASTM A666, the material it is not magnetic, has greater resistance to corrosion, and it increases its strength at higher temperatures.
2. Components drawings follow ISO 1000 standards in order to streamline the manufacturing process

4.4. Prototype Assembly

4.4.1. Mechanical

A list is provided below to summarize the step-by-step procedure followed to manufacture the inspection vehicle.

1. Print Housing for the motors on FlashForge Creator 3D printer:

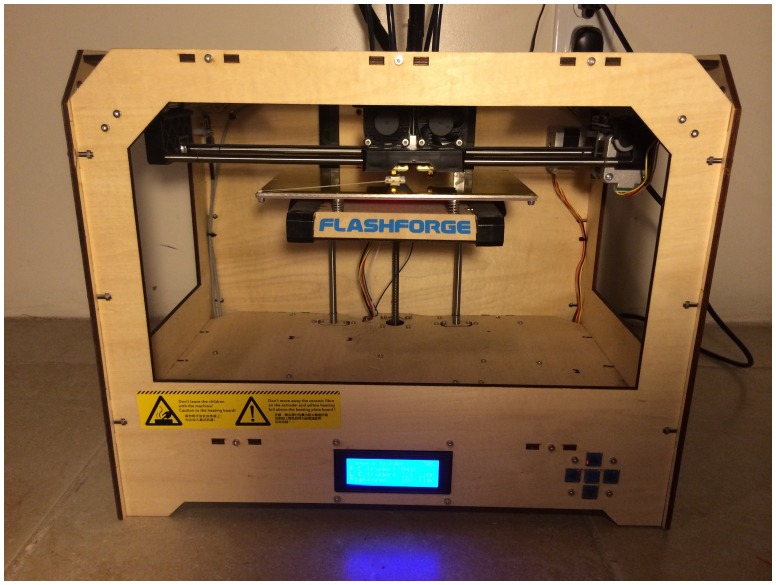

Figure 23. 3D printer using Flash Forge Replicator.

- Use a Replicator to print the housing in two parts.

- Use replicator G to generate the G code for the printer.
- Print the parts with full support and without support.
- The full support requires extra grinding to smooth out the sides. The gaps within the part are small enough to print without support and not affecting the integrity of the part.

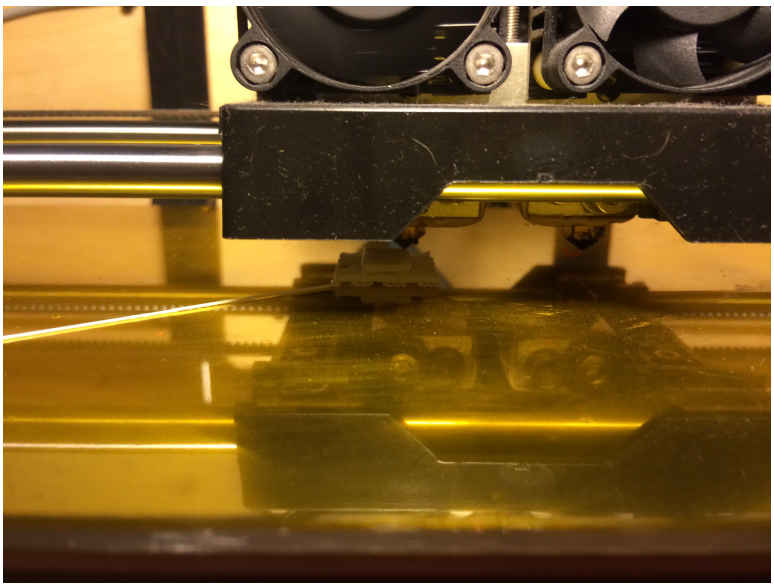

Figure 24. A view of the 3-D printing of the frame.

2. Grind off plastic from the housing to fit the motors:
   - Even though the housing is printed within tolerance of the motors the printer itself is limited to a certain resolution.
   - Due to the size of the parts being assembled the 3D printer is working at its maximum resolution.

3. Drill holes on the plastic wheels and use glue and rubber eraser for bushings:

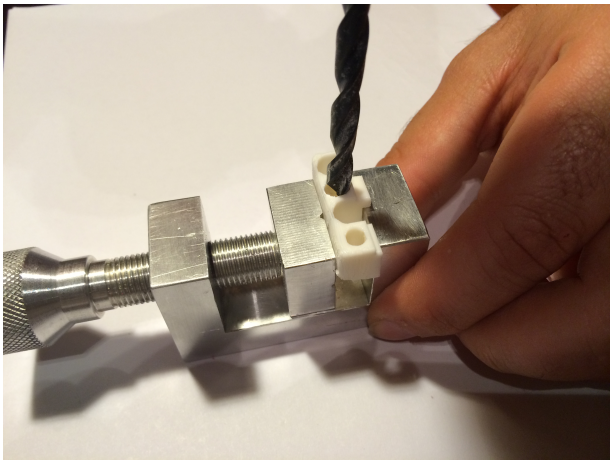

Figure 25. Drilling holes into frame using a vice for support.

- The wheels that were used did not have the pre-drilled holes of 1 mm.
- Need to purchase wheels with pre-manufactured wholes of 1 mm or purchase a drill bit of 1 mm to make holes.

4. Solder the ground and power supply to each independent motor:
   - Spliced the 30 gauge copper cables and put solder at the tips.
   - With the use of a vice grip holding the housing and a magnifying glass to see what we were doing we soldered the copper wire to the motors.

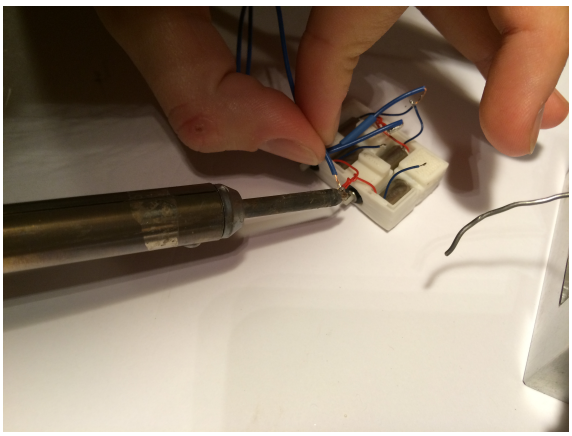

Figure 26. Using a soldering gun to solder the power cables to the motors.

5. Fit the wheels into the shaft of the motor and add crazy glue to secure it in place:
    - Clean the motor shafts and the wheel hole.
    - Put a small amount of glue into the shaft motor and stick the wheel inside.
    - Wait a few minutes and make sure the glue dries.

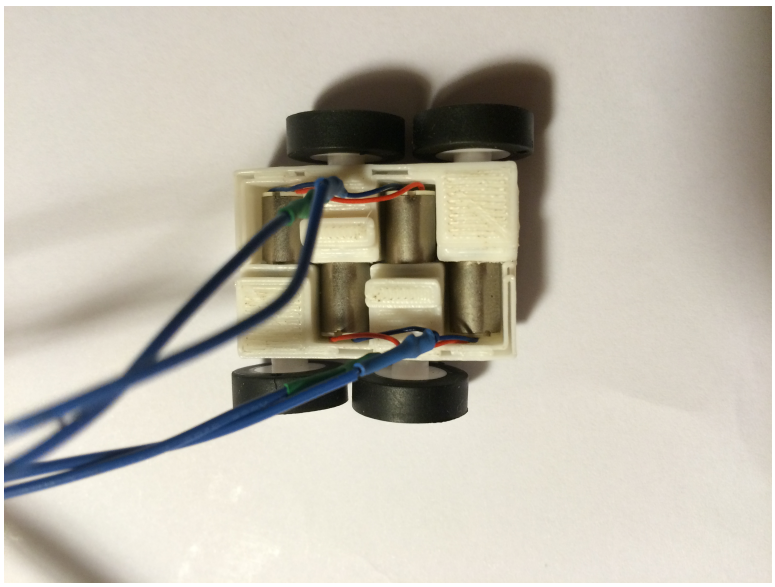

Figure 27. Wheels attached to the motor shaft.

6. Glue the camera holder to the frame and glue the camera to the camera holder:

- Using the 3-D printer, print the camera holder and glue it on the bottom of the frame of the vehicle.
- Take the front of the camera and glue it into the space the camera holder provides.

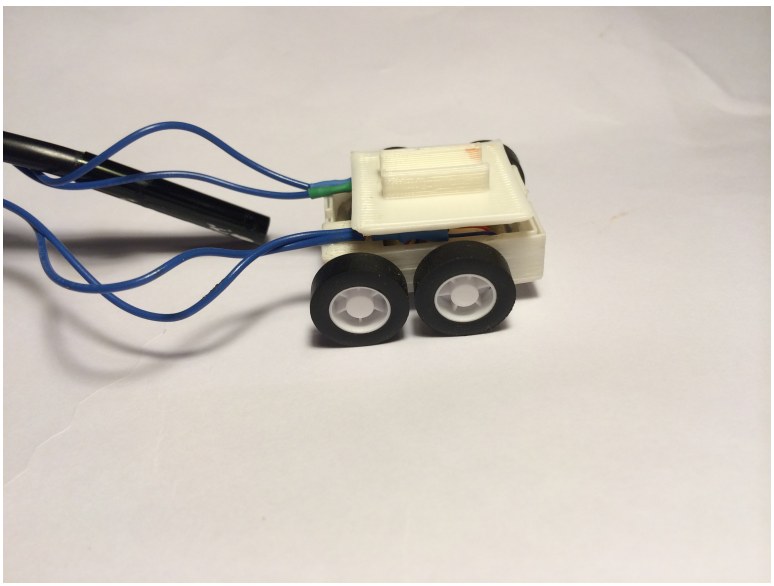

Figure 28. Camera holder glued to the bottom of the frame.

7. Rap the tether with electrical tape to have a single cable traveling through the channel:
   - Take the electrical tape and with an assistant rap the electrical tape around the entire tether length.
   - Make sure you rap the electrical in the position that makes the tether as smooth as possible to decrease frictional force.

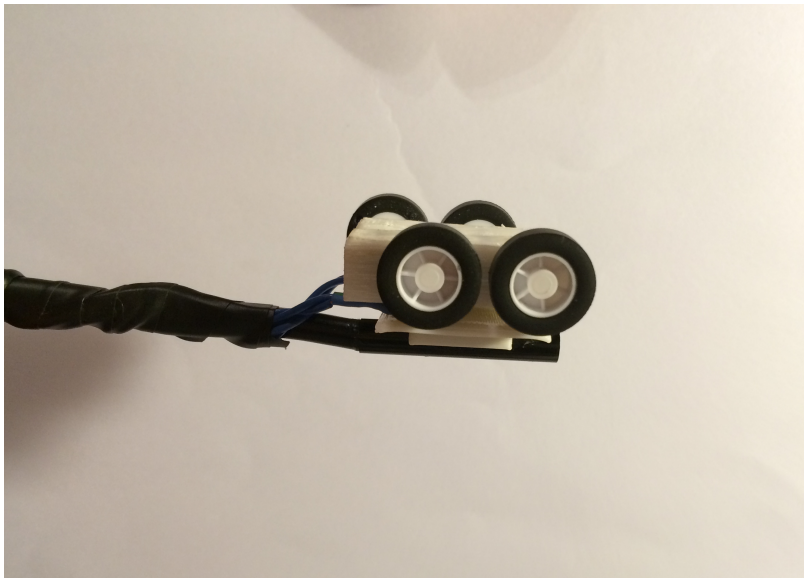

Figure 29. Camera glued in place and electrical tape raped along the tether length.

4.4.2. Electrical

4.4.2.1. Power Source

As seen in Figure 30, initially we started with a 9 V alkaline battery to power the inspection vehicle.

Figure 30. Alkaline Battery

When powering the inspection vehicle we noticed that we could not maintain a constant current supply. As the inspection vehicle asked for current, the voltage would drop significantly

after two trials and the battery had to be replaced because the current supplied to each motor was changing over time for each trial as seen in Table 2.

Table 2. Voltage Drop

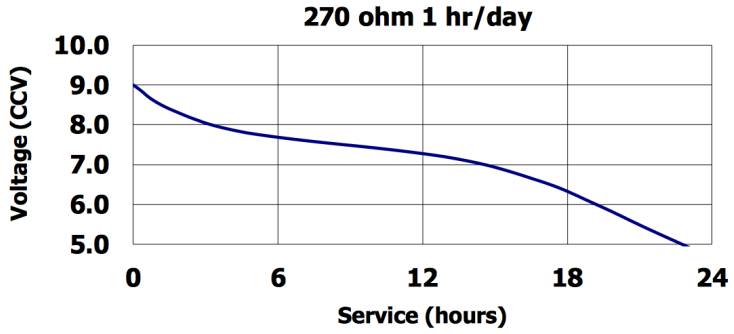

As per Table 3, at 400 mA the inspection vehicle could maintain that current at 6 V. As trials continued as seen in Table 2, the voltage would drop and the results were inconsistent thus it was concluded an alternative battery source was required that could maintain a constant voltage and supply the inspection vehicle with enough power for multiple trials.

Table 3. Constant Current Performance

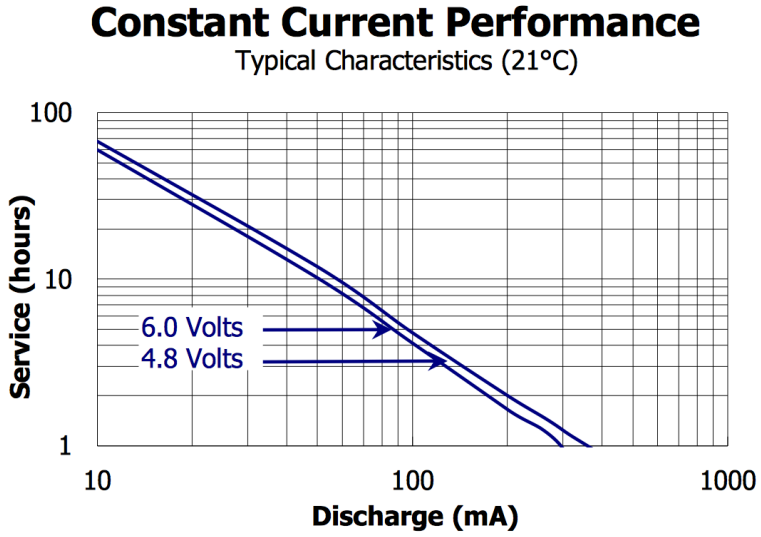

After much research we decided to use an external lead acid battery supplying 12 V to the circuit as the inspection vehicle's source. A battery that can supply higher than 500 mA of constant current to the inspection vehicle while still being able to go through the channel

multiple times for thorough testing. The battery used was an Enercell 12V/ 5AH sealed lead acid battery with FI connectors as seen in Figure 31.

Figure 31. Lead Acid Battery

Even though they have a low energy to weight ratio they can supply high surge currents meaning that the cells have a large power to weight ratio. Since we decided to have an external battery source the weight of the battery was not an issue. The battery can be recharged multiple times and serves as a reliable constant voltage source.

4.4.2.2. Microcontroller

The microcontroller used for this project is an Arduino Uno as shown in Figure 32. It is a board-based controller with an ATmega328 processor. It is an open source allowing it to be compatible with the multiple sensors and devices used in the project. It has fourteen digital input/output pins of which six can be used as pulse width modulation (PWM) outputs.

Figure 32. Arduino Uno

Five out of the six analog input pins were used to monitor the currents supplied to each motor and to control the speeds being generated in each motor.

The maximum output voltage from each pin is 5 V and the maximum current that each pin can handle is 40 mA. This creates a problem if used directly because each motor needs at least 70 mA of constant current to be able to drag the tether on the refractory pad at 4.87 m.

In order to be able to provide that kind of power to the inspection vehicle an H-bridge was needed. An L293D H-bridge as shown in Figure 33, was used as it has a maximum output voltage of 36 V and a maximum current of 2 A. The direction of the motors are controlled by the digital pins and the current being supplied to the inspection vehicle is controlled by two PWM pins connected from the Arduino to the bidirectional H-bridge module.

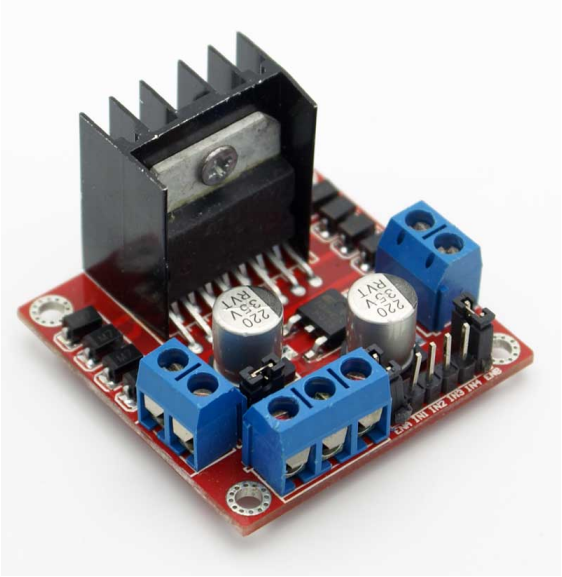

Figure 33. L298 H-Bridge

The supply to the H-Bridge is 12 V however each transistor that it goes through has a 1.5 V drop. Because it has a double transistor for bidirectional motion there is a 3 V drop. Therefore the maximum output from the current source being supplied to the inspection vehicle is 9 V. Part of those 3 V is being lost to heat which is why the H-bridge comes with an aluminum heat sink to dissipate the heat. The H-bridge is controlled by the two Arduino PWM pins which regulate the output voltage from 0 to 9 V.

To keep the H-Bridge from providing too much current we mounted two hall effect current sensors for each side of the inspection vehicle. The sensor can sense up to 5 A at a sensitivity of 180 mV/A. [24]

Table 4 below was used to calibrate the sensors in order to provide an accurate current reading. They are used to restrict the current supply to the motors to keep them from burning out. Based on the maximum tested, the stall current of the motors is 150 mA per motor.

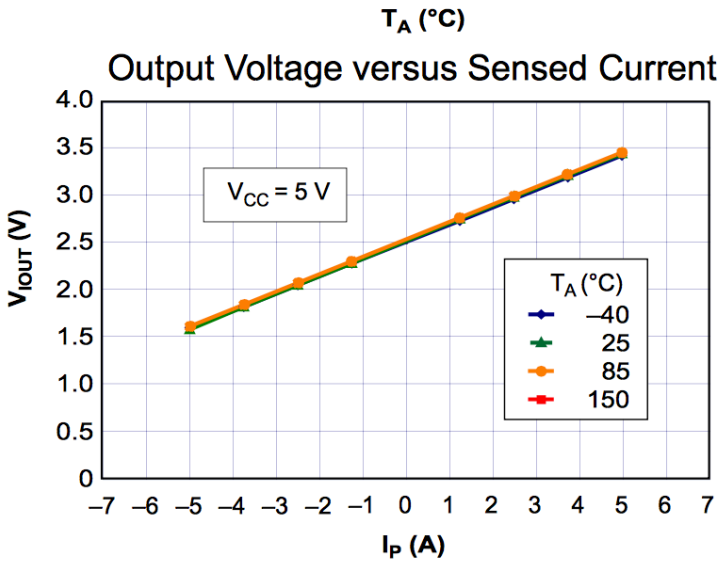

Table 4. Output Voltage vs. Sensed Current

4.4.2.3. Controls

The speeds for two 50 kΩ resistors control the inspection vehicle connected to the Arduino. The Arduino converts the analog input of 0 to 5 V from 0° to 300°. The Arduino receives the signal from the current sensors and the potentiometers and then allows the speed of the inspection vehicle to increase as long as the current does not exceed 150 mA per motor.

The potentiometers as seen in Figure 34, have a tolerance of 20%, which is the reason why we have to monitor the voltage through the Arduino by having a serial communication between the laptop and the Arduino.

Figure 34. B50K Potentiometer

4.4.2.4. Wiring

The inspection vehicle has a tether, which allows for both communications with the camera and driving of the motors. We used 30 AWG stranded copper wire in order to minimize the weight of the tether and generate a smaller pulling force so that the inspection vehicle to be able to reach the 4.87 m. According to the ASTM standard specification for standard wire as shown in Table 5, the ratings of 30 AWG stranded wire is 103.2 Ω/ 304.8 m and a maximum current of 182 mA.[25]

Table 5. Power Transmission Cable

Wire Gauge	Resistance (Ohms)/1000 ft	Max Current (mA)
30	103.2	182

There are four power transmission cables that allow us to control the inspection vehicle while inside the channel. Each side is controlled by two of the cables. Due to the amount of current through the wire there had to be two grounds to distribute the currents separately. According to Table 5, the resistance on each cable will be about 1.75 Ω. Even though the resistance is small there is still power losses due to the cable resistance that needs to be taken into consideration. On each wire there is a loss of 0.45 W at a maximum current of 150 mA. Because the wire gauge is so small the breaking force had to be taken into consideration. Since the cable is being used as a tether the maximum pulling force on each wire at any given time is 12.23 N.

5. Proof of Concept

The primary concept of this project was to implement a magnet into a small vehicle that could travel through a 3.81 cm by 3.81 cm channel. This concept became feasible with the use of a magnet block attached to the top of a frame containing four motors attached to four wheels. The initial proof of concept was analyzed when the magnet from K&J Magnetics, motors and wheels arrived. The frame was printed and the vehicle was assembled. The initial proof of concept was deemed a success when the motors provided enough torque that the car moved forward and the magnets provided enough force to hold the vehicle upside down. Figure 35 shown below shows the vehicle traveling upside down in the middle of the channel.

Figure 35. This picture shows a snapshot of the vehicle running along the channel upside down.

The second phase of the proof of concept was to analyze if the device could pull the tether at least 4.87 m into the channel giving visibility of 45% of the tank bottoms at Hanford Site. This phase of the proof of concept was also deemed a success when the device was positioned at 4.26 m and pulled the tether for 0.61 m.

Figure 36 shown below shows this final proof of concept.

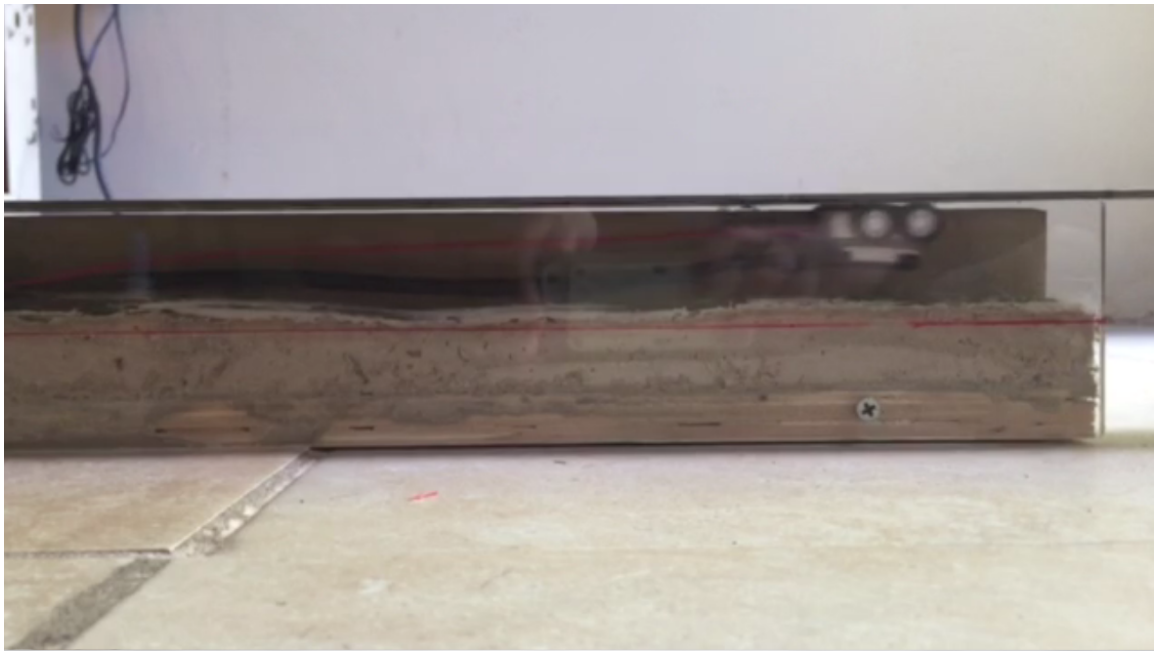

Figure 36. This picture is a snapshot of a video showing the device reached the 4.87 m.

The vehicle ultimately traveled from 0 to 4.87m in approximately 40.4 seconds at an average velocity of 0.123 m/s.

6. Analysis

There are two constraints that drive the vehicle's design and capabilities: (1) the vehicle's ability to pull the weight of the tether as it travels through the refractory pad channel and (2) the force of the magnet required to hold the vehicle to the top of the tank.

6.1. Torque Analysis

The tether supplies the power for the motor as well as the camera feed for live visual feedback. As the vehicle travels through the refractory pad channel, when the distance increases the weight of the tether increases as well. Our proof of concept lies on first determining the maximum torque required to pull the maximum force. Defining the maximum torque required then enables us to find a motor that fits within the space constraints that can also provide the specified torque.

This idea is based on a static analysis relating the wheel diameter, force and torque. By knowing the force required and the wheel diameter, one can easily calculate the torque required as seen in Equation 1 and visually explained in Figure 37. [23]

Equation 1. Torque Equation

$$T = Fr$$

Where T = Torque to be supplied by the motor [mN-m]

F = Force created by tether friction [N]

r = Radius of Wheel [m]

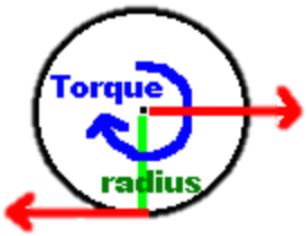

Figure 37. Torque = (Force) (Radius)

The first step was determining the maximum force required. To identify the force, the tether was laid over the refractory material experimental set up as seen in Figure 38.

Figure 38. Tether over refractory material

The channel was then lifted at a slow constant pace up as seen in Figure 39.

Figure 39. Lifting channel

The tether line was observed as the channel was lifted and when the tether would eventually slide back, the channel was held at that position and the angle between the channel and the floor was calculated. An example of how the angle was determined using a photo protractor can be seen in Figure 40.

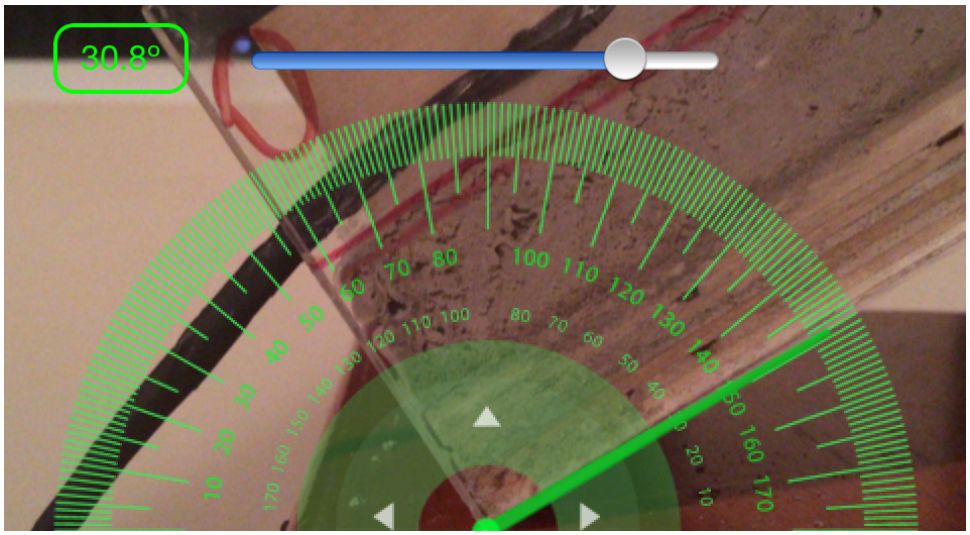

Figure 40. Protractor Photo

Ten trials were completed and Table 6 below displays the data collected for the different angles measured of each trial with an average of 30.66° and a standard deviation of 2.07 was calculated in order to see the accuracy of our measurements. We concluded that the standard deviation was appropriate for the range of error that we were expecting to have.

Table 6. Angle Data

Trial	Angle (°)
1	28.3
2	27.5
3	29.2
4	30
5	31.7
6	34.2
7	30.8
8	30.8
9	30.8
10	33.3
Average	**30.66**
St. Dev	**2.07**

Next, as seen in Equation 2 and graphically represented in Figure 41, a static analysis to calculate the sum of forces in the x direction allowed us to calculate frictional force created by dragging the force along the refractory material.

Equation 2. Sum of Forces in X - Direction

$$F = mgsin\theta$$

Where F = Force created by tether friction [N]

m = Mass of tether [kg]

g = Gravitational Acceleration [m/s^2]

θ = Angle [°]

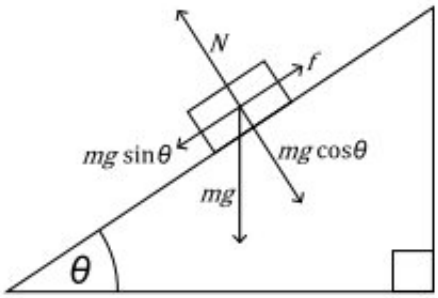

Figure 41. Sum of Forces in X - Direction

The mass of the tether was weighed at 0.23 kg and the gravitational acceleration is 9.81 $\mathrm{m/s^2}$ and using the average angle as given by the data at 30.66°. This gave a maximum force of 1.15 N.

Finally based on the space constraints within the channel, it was concluded that the maximum radius for wheel was 0.007m thus multiplying this by the calculated force gave a required torque of 8.03 mN-m. This is the torque required by the motor in order to pull the tether through the refractory material up to 4.87 m.

6.2. Magnet Analysis

Secondly, the force of the magnet to hold the vehicle up against the tank as it travels through the refractory pad channel must be greater than the weight of the magnet as well as the downward force of the tether as explained in visually represented in Figure 42.

$$F_m \geq F_w + Fsin\theta$$

Where F_m = Magnetic Force [N]

F_w = Weight of the Vehicle [N]

F = Force created by tether friction [N]

θ = Angle [°]

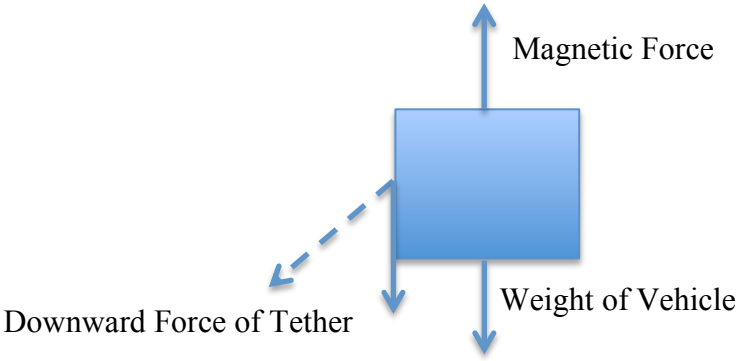

Figure 42. Sum of the Forces in the Y-Direction

The weight of the vehicle was measured at 0.15 N while the tether force was known at 1.15 N, the angle to determine was downward force was proved to difficult and so it was assumed that the magnet had to be greater than the total weight and total tether frictional force giving a total of 1.3 N. The magnet also has a size restriction of 2.54 cm by 2.54 cm in order to fit on top of the vehicle without interfering with the wheels and a maximum thickness of 0.28 cm in order to leave clearance between the magnet and the top of the tank so that the vehicle did not have to overcome the frictional force of the magnet sliding against the tank.

Three different magnet sizes and thicknesses were considered that could be applicable for the vehicle as seen in Table 7 reference from Figure 43, Figure 44, and Figure 45 as provided by K & J Magnetics calculator based on the distance from the tank. [26]

Table 7. Magnet Graph

Magnet	Length [cm]	Width [cm]	Thickness [cm]	Distance from Tank [cm]	Force [N]
BX0C1	2.54	1.27	0.079	0.216	2.09
2 X BX0801	2.54	1.27	0.158	0.137	8.8
BX0801	2.54	1.905	0.158	0.137	12.32

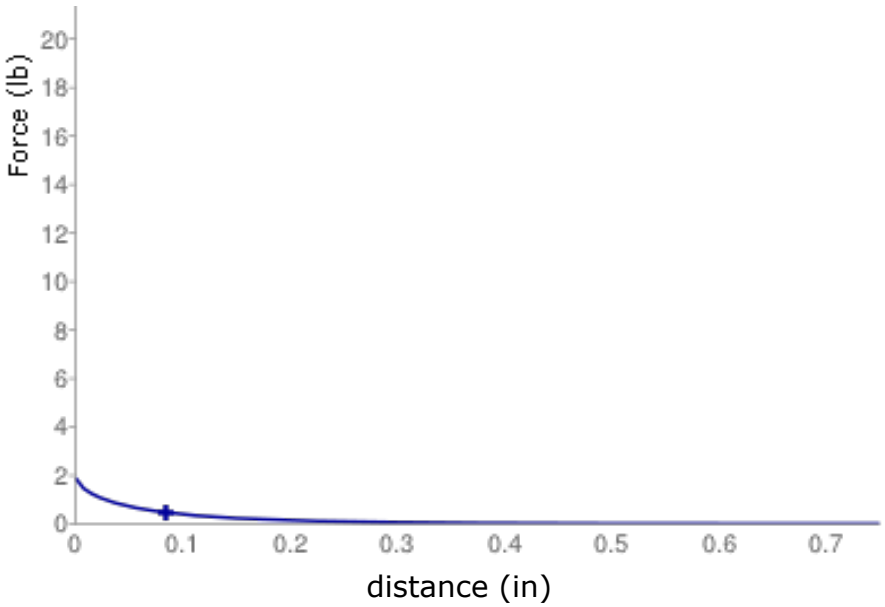

Grade = N42
Length = 1in
Width = 0.5in
Thickness = 0.03125in
Distance = 0.08528in

0.47 lb

Figure 43. BX0801 Magnetic Force at 0.216 cm from Tank

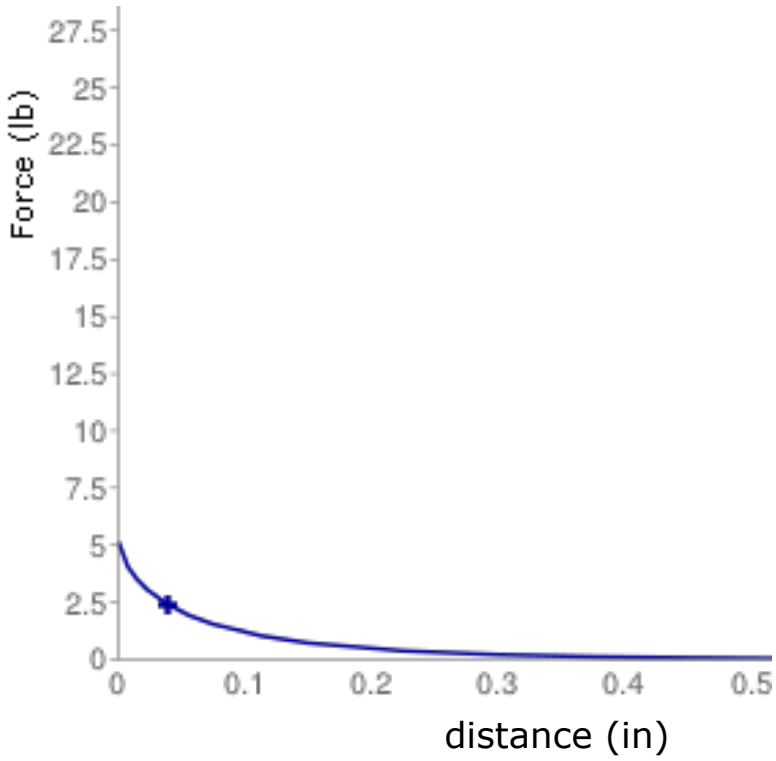

Grade = N42
Length = 1in
Width = 0.5in
Thickness = 0.0625in
Distance = 0.054in

1.98 lb

Figure 44. Two BX0801 Magnetic Force at 0.137 cm from Tank

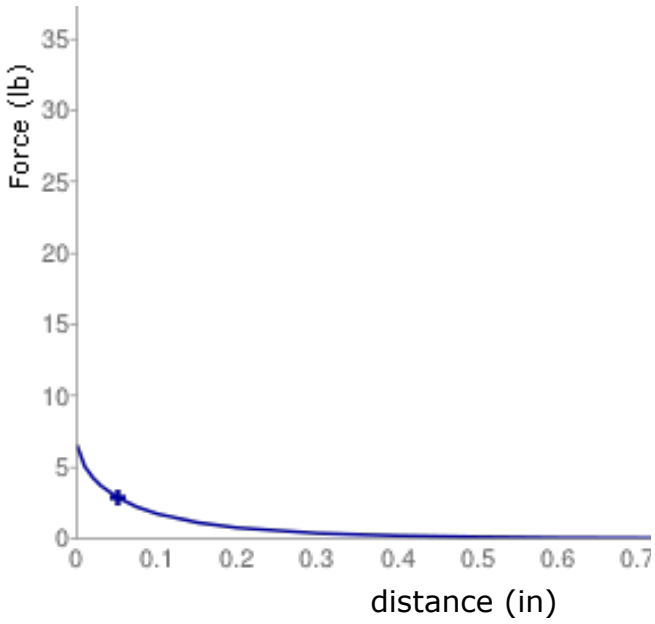

Figure 45. BX0C1 Magnetic Force at 0.137 cm from Tank

6.3 Statistical Analysis

In order to determine the amount of trials to perform to determine that the experimental speed of the device acquired is accurate, we will utilize the normal-z distribution method for statistical analysis. This method uses Equation 3 to determine the number of samples needed to be collected to reach the desired margin of error or less.

Equation 3. Sample Size

$$n = \left(\frac{z_{\frac{\alpha}{2}}\sigma}{E}\right)^2$$

Where n = sample size

$z_{\frac{\alpha}{2}}$ = Confidence level constant

E = Margin Error

σ = Standard Deviation

As required by the formula, a standard deviation value is needed to obtain the sample size required to reach the desired margin of error required. Usually the standard deviation is determined from previous studies and/or experimental data. However, due to the nature of this research, this method of finding deviation it is not feasible. In order to be able to utilize the formula above, three trials were completed to record the velocity of the device when the medium strength magnet was attached to it. After the three trials were completed, the average and deviation were tabulated as seen in Table 8.

Table 8. Medium Magnet Trials for Statistical Sample Size Determination

Medium Magnet (Initial Trials)	
Trial #	Velocity (cm/s)
Trial 1	25.25
Trial 2	23.94
Trial 3	21.459
Average	23.549
Standard Deviation	1.925

Using Equation 3, standard deviation of 1.925, confidence level critical value of 1.96, and margin of error of 1, a minimum sample size of 14.162. This value was rounded to a minimum

sample size of 15. The values for standard deviation, confidence level value, and margin of error were assumed. [27]

7. Testing

7.1. Velocity

It is important to determine the velocity of this device. For this reason, tests were created to determine the velocity of the device with different magnet strengths attached to it. The set up for this test is shown in Figure 46. As can be seen, we positioned the device on a carbon steel plate and put markers from 0 to 100 cm at 10 cm increments. This gave us enough points to determine a constant velocity for the device. The different magnets were used to determine the effect of the magnetic force on the torque of the motor. Measuring the speed and utilizing the motor specification graph we found the required increase in torque for each increasing magnetic force.

Figure 46. Speed Test Set Up

With a stopwatch we measured the time it took for the device to travel each measuring mark until it reached 100 cm. There were five trials for the low and high magnet strength and fifteen trials for the medium magnet strength. Fifteen trials were completed for the medium magnet strength because after completing the statistical analysis as mentioned previously, it was determine that a minimum of fifteen trials were needed in order to obtain accuracy in the our results. For lack of time and equipment we decided to complete the fifteen trials for the medium

strength magnet which we determined as the magnet that was the most feasible for our design. Also, these tests were completed providing the device with 7.23 V for every magnet strength and every trial. The voltage needed to be constant in order to later compare the values obtained per magnet strength accordingly.

As seen in Figure 47, a Distance vs. Time graph line was created for each of the 5 trials and the average was also calculated. Additionally, we determined the best fitted straight line for the average plotted points and determined the velocity by finding the slope of the line. The velocity for the low magnet strength is 37.024 cm/s with a calculated standard deviation of 0.775 cm/s giving certainty in the test results. This is the velocity that the device can run at free load; without pulling the tether. It can also be stated that this is the velocity the device will have at the beginning of the channel. As the device starts pulling the tether there will be an increase in torque and the velocity will decrease until the maximum torque is reached and the device comes to a stop.

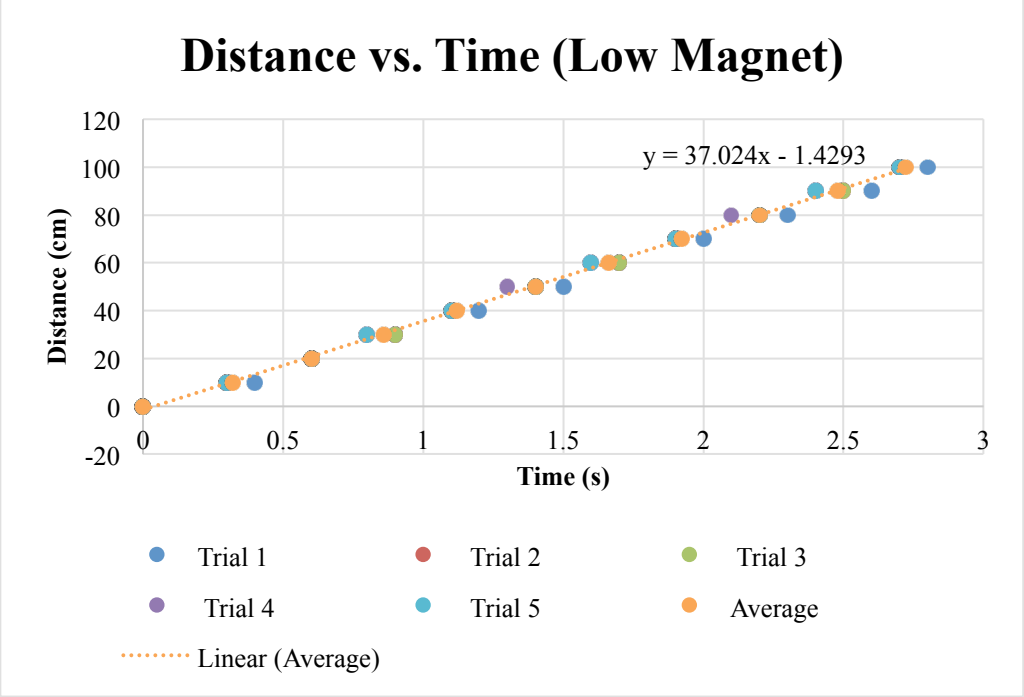

Figure 47. Distance vs. Time for Low Strength Magnet

Additionally, the Distance vs. Time for the medium magnet strength was plotted in Figure 48. In this case, there were fifteen trials of data collected due to the statistical analysis as mentioned earlier. In the analysis section it was discussed how using statistical analysis the sample size was calculated to be at least fifteen trials. Due to time and resource constraints, it was decided that this amount of trials was only be done with the medium magnet as this was the magnet chosen for our final design. The velocity for the medium magnet strength is 22.942 cm/s and a standard deviation of 1.439 cm/s was calculated giving certainty in the test results. This is the velocity that the device can run at free load; without pulling the tether. As mentioned before, this is the velocity the device will have at the beginning of the channel.

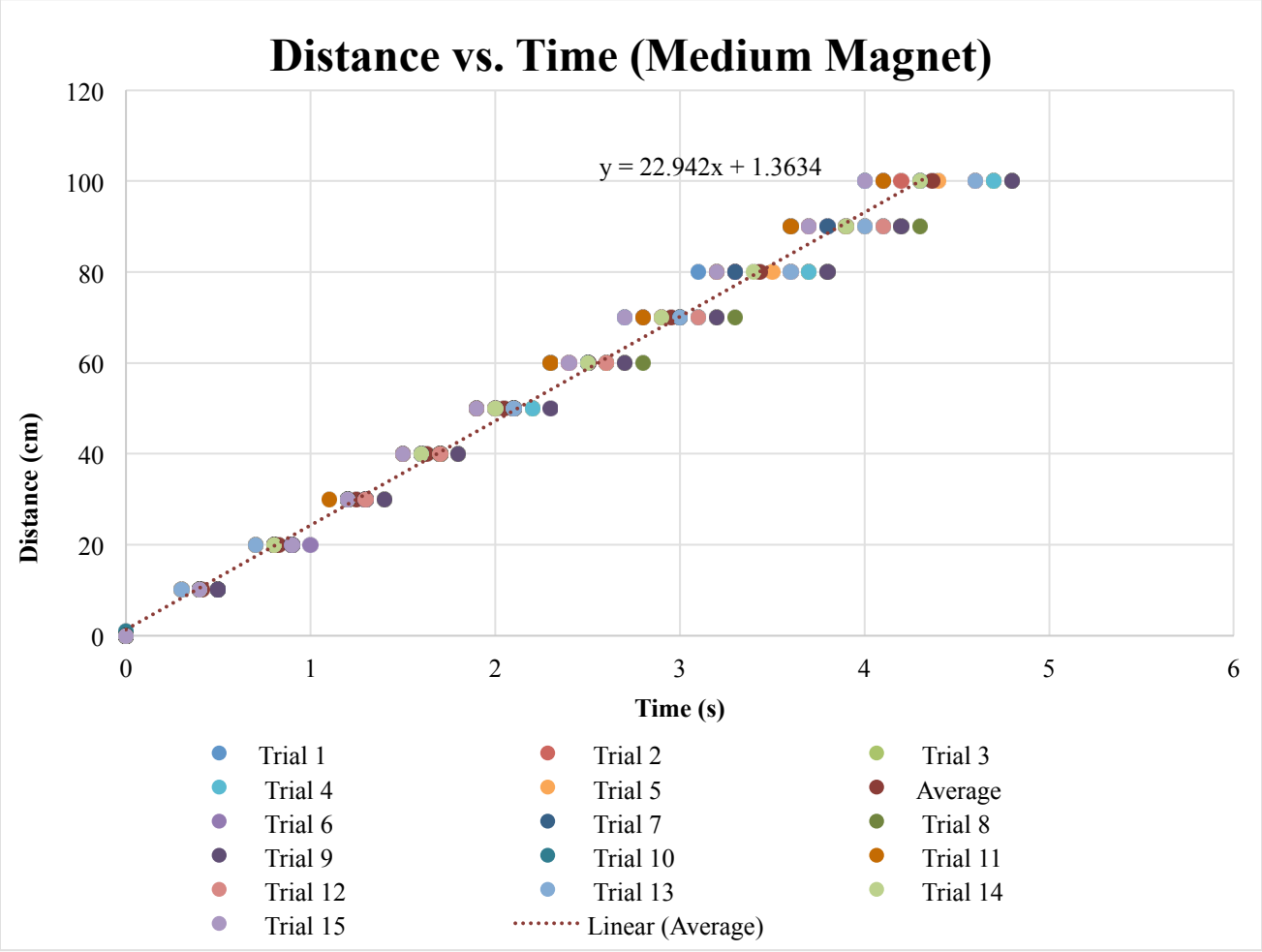

Figure 48. Distance vs. Time for Medium Strength Magnet

Finally, the Distance vs. Time for the high strength magnet was graphed in Figure 49. The average was calculated using five trials and the velocity was found from the slope of the best fitted line. The velocity of the device with the high magnet strength attached is 18.887 cm/s and a calculated standard deviation of 2.66 cm/s gave certainty in the test results.

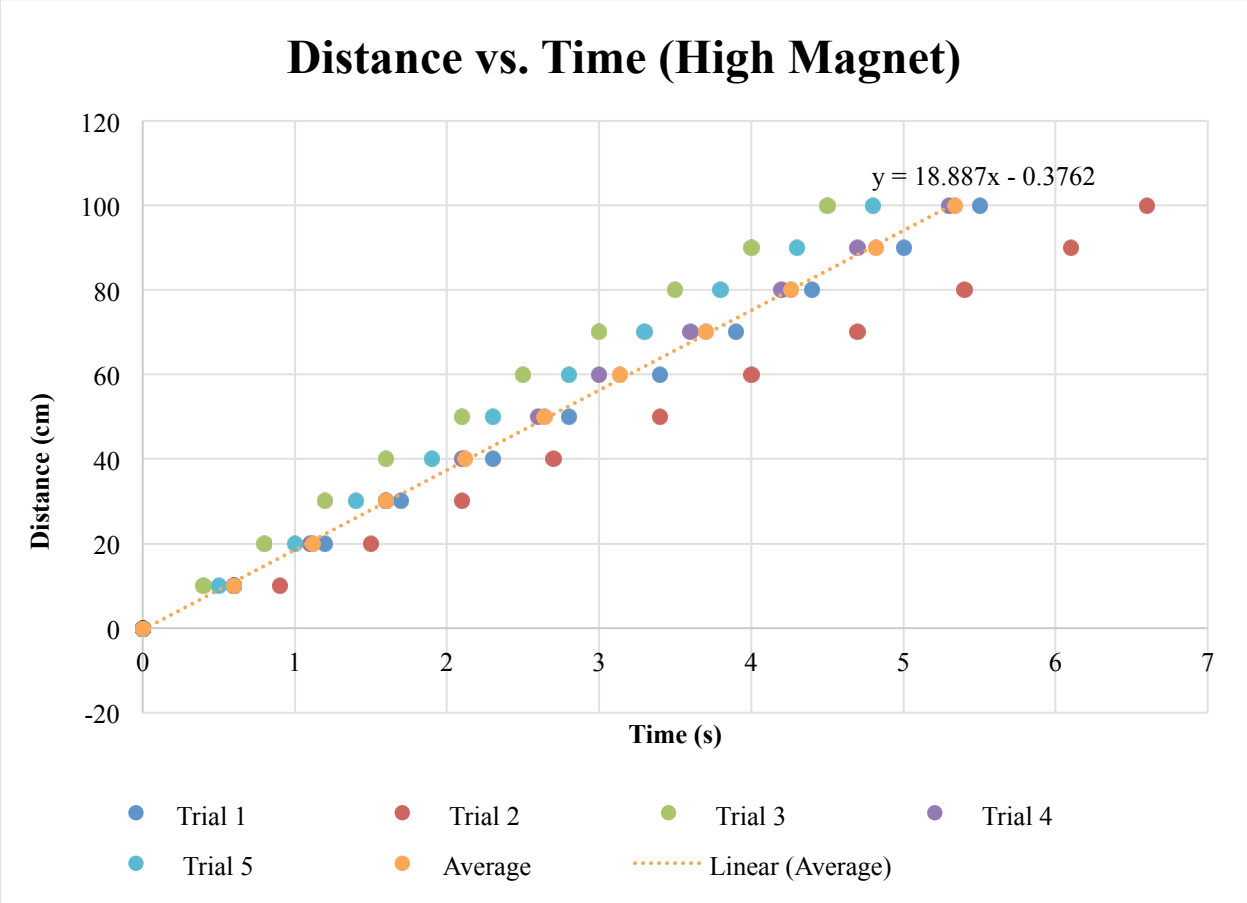

Figure 49. Distance vs. Time for High Strength Magnet

From these calculations it was determined that as the magnet strength increases so does the standard deviation. When performing the tests, it was observed that the motors would get increase in temperature after each consecutive trial as we increased the magnet strength. Because of this, it is concluded that the magnet strength should be just the necessary amount to hold the magnet upside down to the steel plate.

Moreover, the average of the Distance vs. Time for each magnet strength was plotted into Figure 50. This figure shows that as the magnet strength increased, the slope of the curve decreased and therefore decreased the speed.

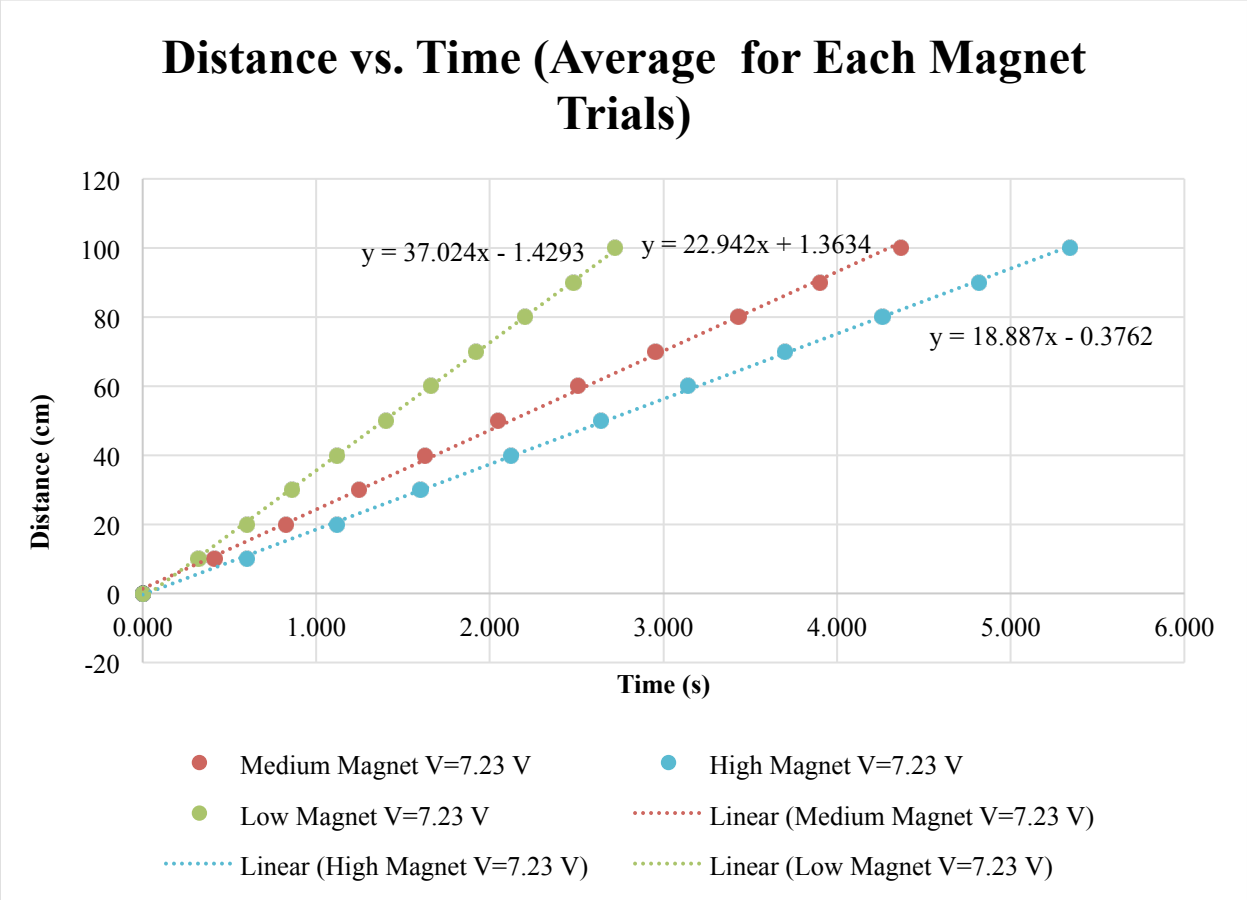

Figure 50.Average of Distance vs. Time at Various Magnet Strength

Lastly, the velocity due to each magnet strength was tabulated in Table 9 and graphed in Figure 51. As shown, there is an exponential decrease in velocity as the magnet strength increases. This shows the relationship between magnet strength and the device velocity. This result is a combination of the effect of the magnet to the motors and the addition of mass to the device as well as decreasing distance from the magnet to carbon steel plate. It was determined that the medium strength magnet was the most feasible to use since it provided enough strength to pull the device against the carbon steel tank and yet still allowed for adequate speed.

Table 9. Velocity at Different Magnet Strengths

Magnet Strength (N)	Velocity (cm/s)
12.322	18.887
8.808	22.942
2.091	37.024

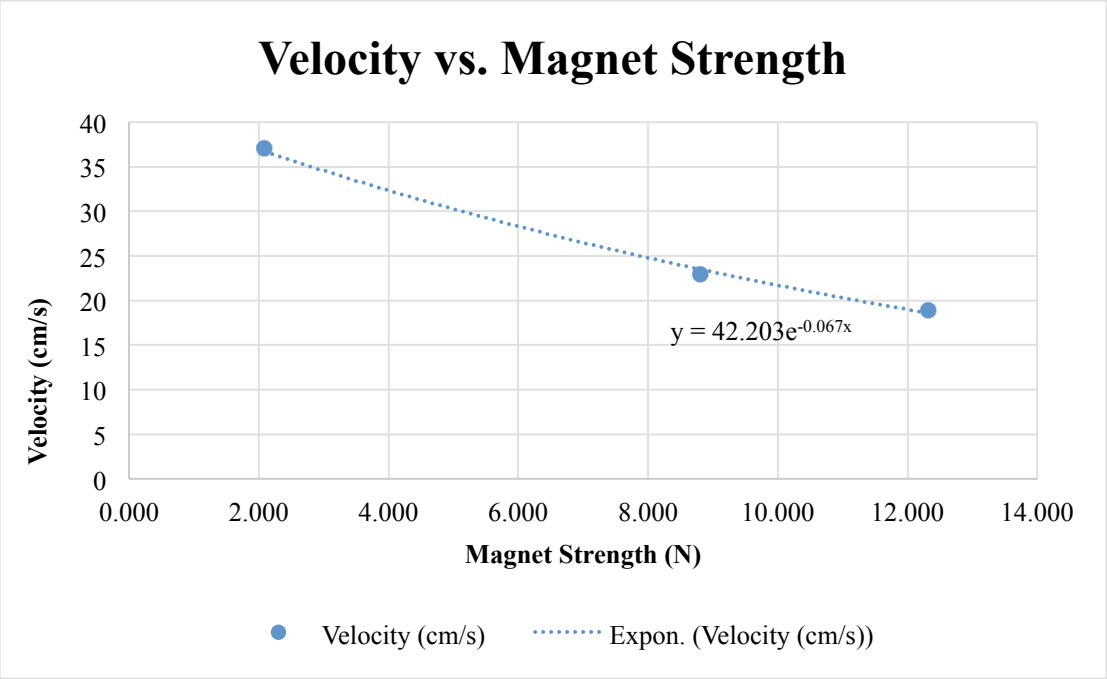

Figure 51. Velocity vs. Magnet Strength

7.2. Torque

The motor test was performed to see if the motors actually had the capacity specified in the Table 10 below.

Table 10. Torque Curve

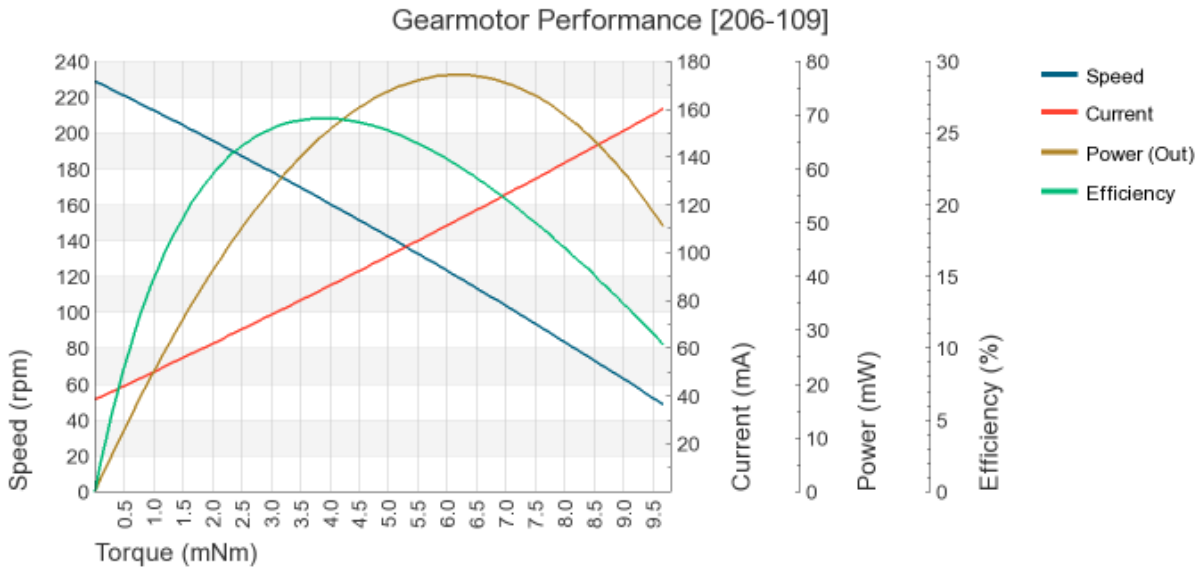

The force required to pull the tether according to our test is 1.73 N. with a wheel radius of $6.99 * 10^{-3}$ m the total torque required to pull the tether is 13.5 mN-m. Since there are four motors the total torque required per motor is 3.375 mN-m. According to the graph above the required current needed to generate a torque of 3.375 mN-m is 85 mA. To be sure that our results were going to be accurate, we needed to test if the motor would be able to generate the torque at the current specified above.

To test this we filled a bag with salt with a load of 0.048 kg. We used a digital hanging scale that has an accuracy of 1 gram to measure the weight of the load that would be used. Since the scale was in English units all units were converted to SI for consistency as seen in Figure 52 below.

Figure 52. Salt Load

The load from Figure 52 above is then tied to the wheel on the motor. If the motor starts to turn once the current of 85 mA is reached then it is generating the necessary torque to move the tether at 4.87 m as seen in Figure 53.

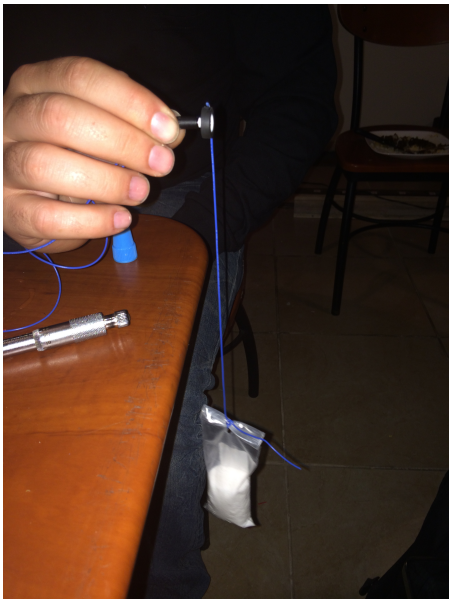

Figure 53. Motor Test

The current was applied to the motor and between 70 mA to 90 mA and the motor began to move. The test was performed multiple times and each time the motor moved the load between 70 and 90 mA.

Since the load curve of the motor went to 150 mA we needed to see the maximum lifting capacity to see how much the motor can lift. At 150 mA the motor was able to lift 0.85 N. At this load the motor is generating a torque of roughly 8.50 mN-m.

8. Project Management

8.1. Timeline

The Gantt chart for the project timeline is shown in Table 11. The major milestones are listed as well as the month and week when the tasks were/are to be completed. For example, starting in first week of January, the literature review began and it was completed by the end of the month. This chart served as a guideline of the ideal schedule of the project and enabled the team to complete the project in a timely and efficient manner. When the schedule was delayed or advanced, this chart was updated accordingly.

Table 11. Project Timeline

Category General	Activity	Month											
		Jan	Feb	Mar	Apr	May	Jun	Jul	Aug	Sep	Oct	Nov	Dec
Project Formulation	Literature Survey	X											
	Conceptual Designs		X										
	Finalized Design			X									
	Cost Analysis				X								
	Material Gathering				X								
	Concept Testing				X								
Prototype Development	System Integration								X				
	Prototype Construction									X	X		
	Prototype Testing										X		
Final Presentation to IAB and MME	Poster Formulation											X	
	Presentation												X

8.2. Team Responsibilities

The general tasks this project comprises of, as well as the team member(s) responsible to complete them, are listed in Table 12. In order to balance the workload the majority of the tasks were shared between at least two members of the group. More complex tasks were divided among three members while tasks that required less effort/time were assigned to a single member. Nevertheless, team members assisted each other in all aspects of the project.

Table 12. Breakdown of Responsibilities among Team Members

Breakdown of Responsibilities			
	Jennifer Arniella	**Daniel Giraldo**	**Gabriela Vazquez**
Global Learning	**X**	**X**	**X**
Solidworks Modeling	**X**		**X**
Literature Review Research		**X**	
Material and Component Selection	**X**	**X**	**X**
Record Keeping	**X**		**X**
Testing Apparatus	**X**	**X**	**X**

8.3. Cost Analysis

In order to determine the final cost of the proposed design, a detailed cost analysis was conducted. As an engineer, it is our job to determine what the lowest possible cost of our project is and it is necessary to research competitive companies that will enable us to reach this goal. After doing research and carefully comparing the information obtained, the components were selected and the final cost is listed in Table 13. Also, the labor cost was calculated using the hours that each team member spends in the project for two semesters and a salary of $12/hour. By adding these two amounts, the total cost of the project is $4,894.16.

Table 13. Cost For Components and Labor Work

Component	**Manufacturer**	**Price/Unit**	**Units**	Total Price
Magnet Plate	KJ Magnetics	$1.98	1	$1.98
Motor	Pololu	$11.95	4	$47.80
Frame (Body)	Printed	$50.00	1	$50.00
Wheels	Pololu	$1.95/pair	2	$3.90
Arduino	Arduino	$49.99	1	$49.99
H-Bridge	Radio Shack	$13.99	1	$13.99
Battery	Radio Shack	$35.50	1	$35.50
Current Sensors	Radio Shack	$10.00	2	$20.00
Potentiometers	Radio Shack	$7.50	2	$15.00
			Total Component Cost	$238.16
Estimated Labor Cost (Spring, Summer and Fall Semester)	Salary	Hours/ Semester	Semesters	Total Labor Cost
	$ 12/hr	388	2	$4,656.00
			Total Project Cost	$4,894.16

To determine the labor cost, the time each member spent on the project is required. Throughout the project development, the time each team member spent on the project was tabulated. The total time spent in the project for one semester is listed in Table 14 along with the specific dates the work was performed.

Table 14. Total Work Hours

Time Reporting							
Group Meetings		Gabriela Vazquez		Daniel Giraldo		Jennifer Arniella	
Date	Time (hrs)	Date	Time (hrs)	Date	Time (hrs)	Date	Time (hrs)
1/27/2014	0.5	1/31/2014	1.5	1/31/2014	3	1/31/2014	1.5
2/3/2014	1.5	2/3/2014	1.5	2/4/2014	1.5	2/6/2014	3
2/10/2014	1.5	2/12/2014	1	2/13/2014	1.5	2/15/2014	1.5
2/26/2014	1.5	2/27/2014	2	2/28/2014	1	2/27/2014	1.5
3/10/2014	3	3/12/2014	2	3/30/2014	2	3/30/2014	1
3/17/2014	2	3/19/2014	1.5	3/21/2014	2	3/19/2014	2
3/24/2014	2	3/27/2014	1.5	3/29/2014	3	3/28/2014	2
3/31/2014	3	3/31/2014	2	3/31/2014	1.5	3/30/2014	1.5
4/7/2014	1	4/10/2014	3	4/12/2014	3	4/14/2014	3
4/14/2014	2	4/16/2014	1.5	4/15/2014	1.5	4/17/2014	1.5
4/21/2014	1.5	4/23/2014	1.5	4/22/2014	1.5	4/22/2014	1.5
8/4/2014	2	8/16/2014	1	8/14/2014	1	8/15/2014	1
8/11/2014	3	8/23/2014	2	8/22/2014	2	8/23/2014	1.5
8/18/2014	3	8/30/2014	2	8/30/2014	2	8/31/2014	1
8/25/2014	3	9/6/2014	1.5	9/7/2014	3	9/8/2014	2
9/1/2014	4	9/13/2014	1.5	9/15/2014	1.5	9/16/2014	2
9/8/2014	3	9/20/2014	2	9/23/2014	1.5	9/24/2014	1.5
9/15/2014	3.5	9/27/2014	3	10/1/2014	1	10/2/2014	3
9/22/2014	4	10/4/2014	1.5	10/9/2014	2	10/10/2014	1.5
9/29/2014	5	10/11/2014	1.5	10/17/2014	2	10/18/2014	1
10/6/2014	4.5	10/18/2014	1	10/25/2014	3	10/26/2014	1
10/13/2014	3	10/25/2014	2	11/2/2014	1.5	11/3/2014	2
10/20/2014	4	11/1/2014	2	11/10/2014	1.5	11/11/2014	1.5
10/27/2014	4	11/8/2014	1.5	11/12/2014	1	11/13/2014	3
11/14/2014	4	11/14/2014	1.5	11/14/2014	1	11/14/2014	2
11/15/2014	6	11/15/2014	2	11/15/2014	1	11/15/2014	1
11/16/2014	6	11/16/2014	3	11/16/2014	2	11/16/2014	2
Total	81.5	Total	48	Total	48.5	Total	47
Total Hours	388						

9. Conclusion

Our main motivation to initiate this project arose from the need to avoid radioactive contamination into the subsurface soil. The Colombia River is located only five miles away from the tanks carrying the radioactive waste and if uncontrollable leakages were to occur the river would be contaminated. This river provides water to the city and could potentially pollute the environment and community in Washington State.

The Department of Energy is in need of specially designed equipment that can travel through the underground tank channel without damaging the refractory pad material. This research design task met the design challenges by creating an inspection vehicle that was able to fit within the small channel size. The design developed consisted of a magnetic plate that will travel upside down along the carbon steel tanks. Testing results concluded that the medium magnet that provided an 8.8 N magnetic force was the best option for the design as it provided enough force to hold the vehicle up as it traveled through the entire channel while not creating overworking the motors to supply a high torque to overcome such a large force. Testing results also demonstrated that the motors provided enough torque for the vehicle to pull the tether throughout the entire channel, although further investigation should be completed to find motors with a greater efficiency and life. The vehicle ultimately traveled within the channel pulling the tether along the refractory pad material from 0 to 4.87m in approximately 40.4 seconds at an average velocity of 0.123 m/s.

In a global perspective radioactive waste management is an issue that all developed countries must address. In order to avoid environmental contamination that can affect the global ecosystem, it is important for us to be proactive in our research towards monitoring and managing waste storage. Our magnetic vehicle is applicable to all countries such as Sweden,

Canada, Finland, and United Kingdom who store waste in a repository that requires periodic inspection or repair. Countries like France, whose nuclear industry is their main supplier of electricity, are working with research companies in a combined effort to develop radiation tolerant robotic devices.

In conclusion, to sustain a safe and dynamic environment in our world today and for future generations to come, there is an obligation to properly treat and store the legacy waste. B.U.G.'s Miniature Motorized Vehicle for the Department of Energy's Hanford Site Underground Channels in a combined effort with international corporations will have a hand to reach this goal.

10. References

[1] "Tank Farms - Hanford Site." *Tank Farms - Hanford Site*. U.S. Department of Energy, 24 Apr. 2014. Web. Mar. 2014.

[2] Engerman, Jason K., Dennis J. Washenfelder, and Kayle D. Boomer. *Remote Evaluation of Hanford Double Shell Tank Primary Tank Bottoms*. Washington River Protection Solutions, LLC, 2013. Print.

[3] Washenfelder, Dennis. "DST Drawing Air Refractory Slots." *Hanford.gov*. Washington River Protection Solutions, 7 Nov. 2012. Web. Mar. 2014.

[4] Dininny, Shannon. "Feds: Nuclear Waste May Be Leaking into Soil from Hanford Site." *NBC News*. The Associated Press, 22 June 2013. Web. Mar. 2014.

[5] Engerman, Jason K., C.L Girardot, D.G. Harlow, and C.L. Rosenkrance. *Tank 241-AY-102 Leak Assessment Report*. Rep. N.p. RPP-ASMT-53793, Rev.0: Washington River Protection Solutions, LLC, October 2012. Print.

[6] "Energy.gov." *Energy.gov*. U.S. Department of Energy, 22 Oct. 2012. Web. Mar. 2014.

[7] Washenfelder, Dennis. "Tank AY-102 Leak Assessment." *Hanford.gov*. Washington River Protection Solutions, 7 Nov. 2012. Web. Mar. 2014.

[8] Washenfelder, Dennis. "Statement of Work, November 2013 VISTA Inspection of AY-102 Annulus Air Channels." *Hanford.gov*. Washington River Protection Solutions, 7 Nov. 2012. Web. Mar. 2014.

[9] *Robotic Technology Selection- Inspection of AY-102 Presentation*. Washington River Protection Solutions, Aug. 2013. Print. Jan. 2014.

[10] Vazquez, Gabriela I., and Dwayne McDaniel. *Subtask 18.2 Monthly Reports*. Issue brief. Miami: Florida International University Applied Research Center, 2014. Print.

[11] Ross, Valerie, “Velociraptor Robots Come To The Rescue.” *Discove*r (2012) : 12,

[12] Kwok, Roberta. “Building Robots That Slither.” *Science News* 182.11 (2012):32

[13] Pratt, Gill A. “Robot to the Rescue. “*Bulletin of the Atomic Scientists.* (2014) :63-69

[14] “Giving Underwater Robots A Firm Grip.” *Machine Design* 84.2 (2012) : 25

[15] http://energy.gov/sites/prod/files/2013/06/f1/DOE-STD-1189-2008.pdf

[16] http://www.astm.org/Standard/standards-and-publications.html

[17] http://www.iso.org

[18] https://www.ieee.org/publications_standards/index.html

[19] *AREVA Hanford AY-102 Presentation*. AREVA Inc North America, Aug. 2013. Print. Jan. 2014.

[20] *Vista Hanford AY-102 Presentation*. Vista Engineering Technologies, Aug. 2013. Print. Jan. 2014.

[21] *IHI Hanford AY-102 Presentation*. IHI Southwest Technologies, Aug. 2013. Print. Jan. 2014.

[22] McDaniel, Dwayne, Tomas Pribanic, Gabriela Vazquez, and Jennifer Arniella. *Conceptual Design of Inspection Tool for AY-102 Refractory Slots*. Rep. no. 2013-P1-M18.2.1. Miami: Florida International University Applied Research Center, 2014. Print.

[23] "How to Build a Robot Tutorials - Society of Robots." *How to Build a Robot Tutorials*. Society of Robots, Nov. 2005. Web. 4 Sept. 2014.

[24] L298 Dual Full-Bridge Driver. *STmelectronics.* Web. January. 2000. <Tech.dma.ac.uk>

[25] ASTM B258 - 02(2008) *Standard Specification for Standard Nominal Diameters and Cross-Sectional Areas of AWG Sizes of Solid Round Wires Used as Electrical Conductors*

[26] http://www.kjmagnetics.com/calculator.asp

[27] http://www.isixsigma.com/tools-templates/sampling-data/how-determine-sample-size-determining-sample-size/

Appendices

Appendix A: Component Drawings

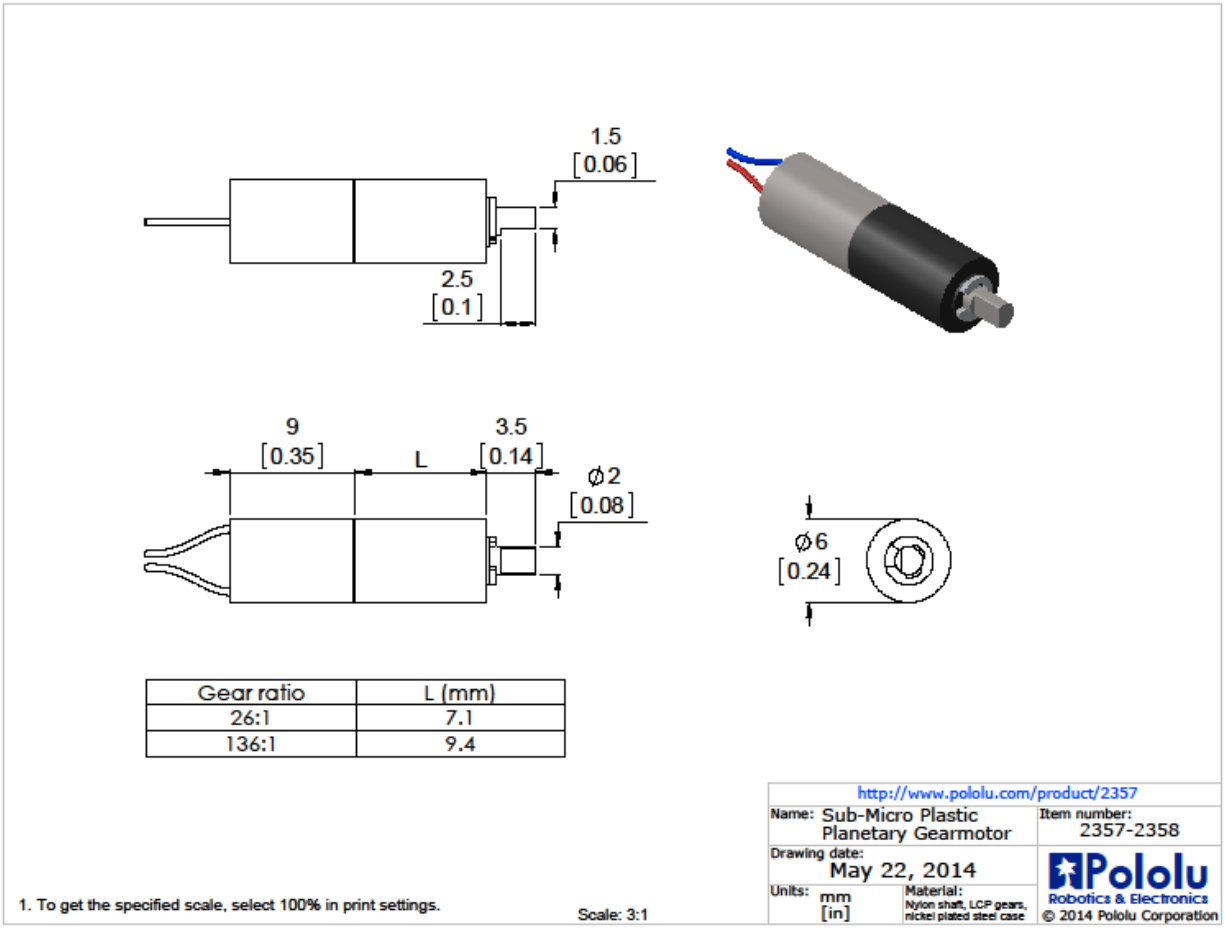

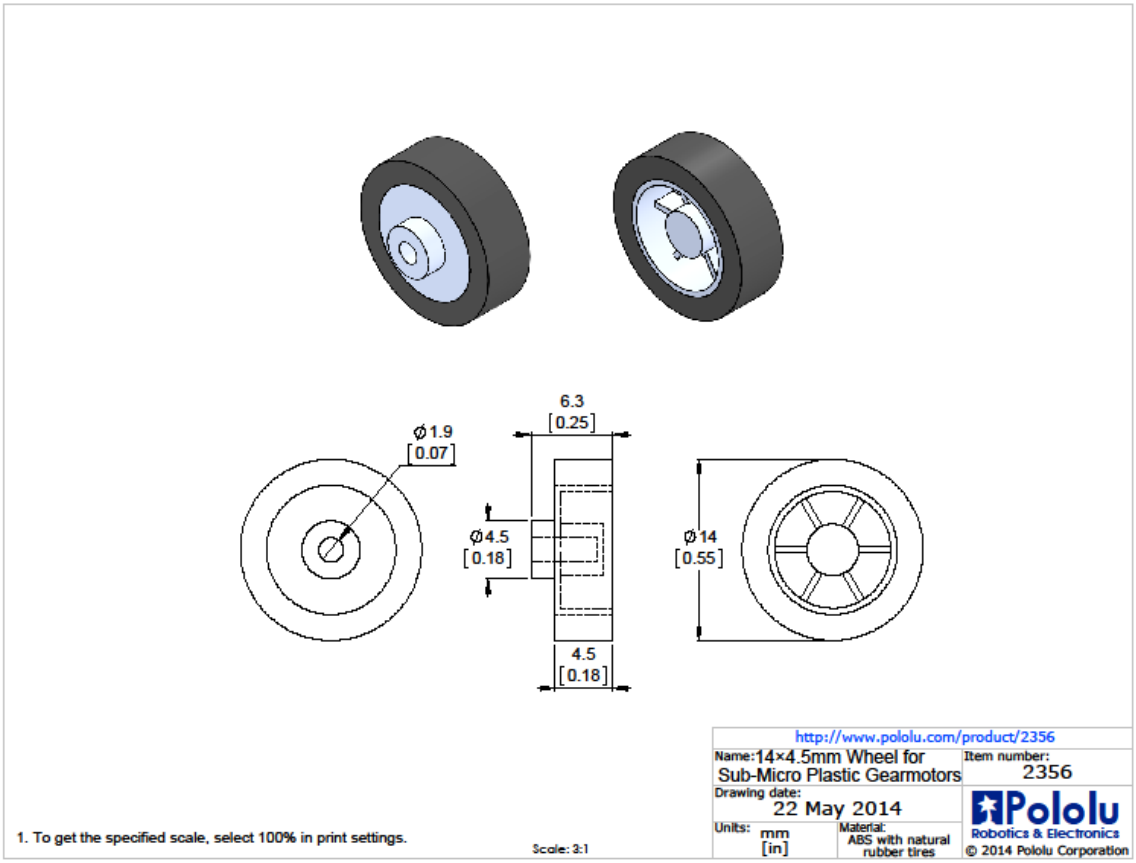

http://www.pololu.com/product/2356

Name: 14×4.5mm Wheel for Sub-Micro Plastic Gearmotors

Item number: 2356

Drawing date: 22 May 2014

Units: mm [in]

Material: ABS with natural rubber tires

Pololu Robotics & Electronics

1. To get the specified scale, select 100% in print settings.

Scale: 3:1

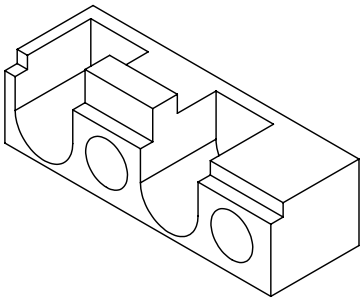

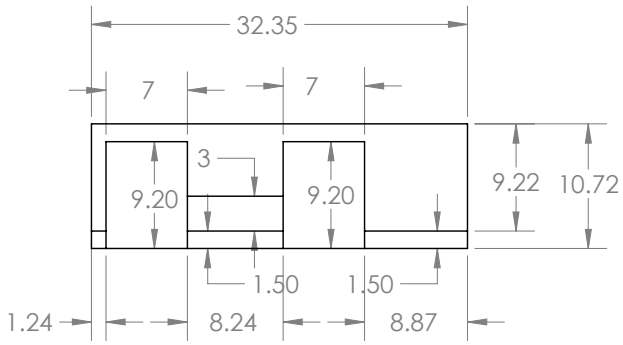

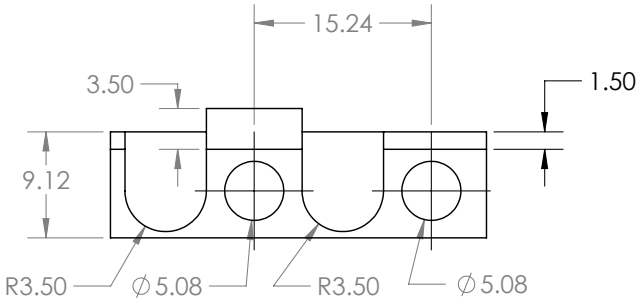

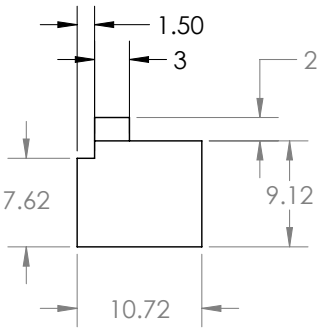

UNLESS OTHERWISE SPECIFIED: DIMENSIONS ARE IN MILLIMETERS SURFACE FINISH: TOLERANCES: LINEAR: +/- 0.001 ANGULAR: +/- 0.001	FINISH:		DEBUR AND BREAK SHARP EDGES		DO NOT SCALE DRAWING	REVISION
	NAME	SIGNATURE	DATE		TITLE:	
DRAWN	Gabriela Vazquez		11/19/14		Frame	
CHK'D	Jennifer Arniella		11/20/14			
APPV'D						
MFG						
Q.A				MATERIAL:	DWG NO.	A4
				ABS Filament	1	
				WEIGHT: 1.71g	SCALE:2:1	SHEET 1 OF 1

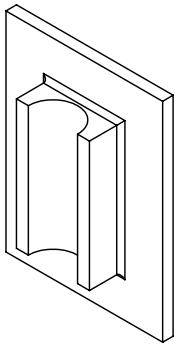

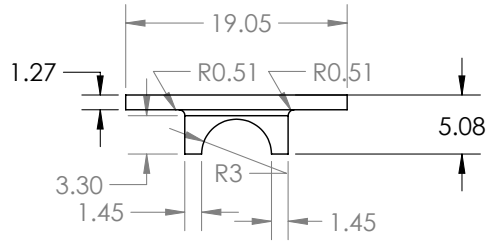

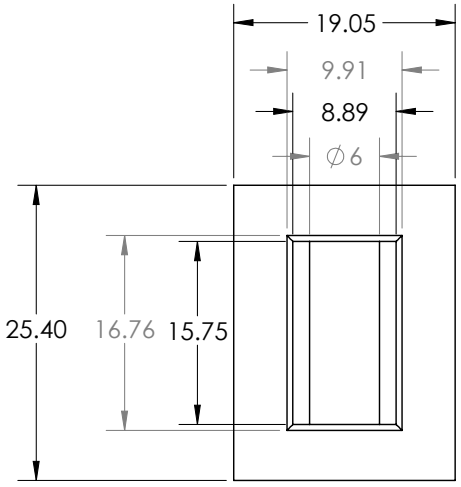

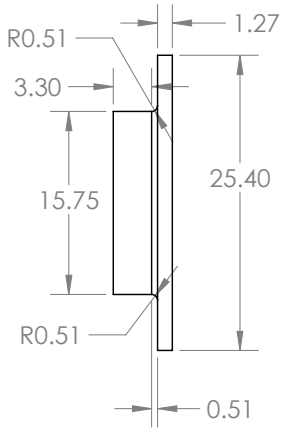

UNLESS OTHERWISE SPECIFIED: DIMENSIONS ARE IN MILLIMETERS SURFACE FINISH: TOLERANCES: LINEAR: +/- 0.001 ANGULAR: +/- 0.001	FINISH:		DEBUR AND BREAK SHARP EDGES		DO NOT SCALE DRAWING	REVISION
	NAME	SIGNATURE	DATE		TITLE:	
DRAWN	Gabriela Vazquez		11/19/14		Camera Holder	
CHK'D	Jennifer Arniella		11/20/14			
APPV'D						
MFG						
Q.A				MATERIAL:	DWG NO.	A4
				ABS Plastic	2	
				WEIGHT: 0.95g	SCALE:2:1	SHEET 1 OF 1

Dimensioned Drawing

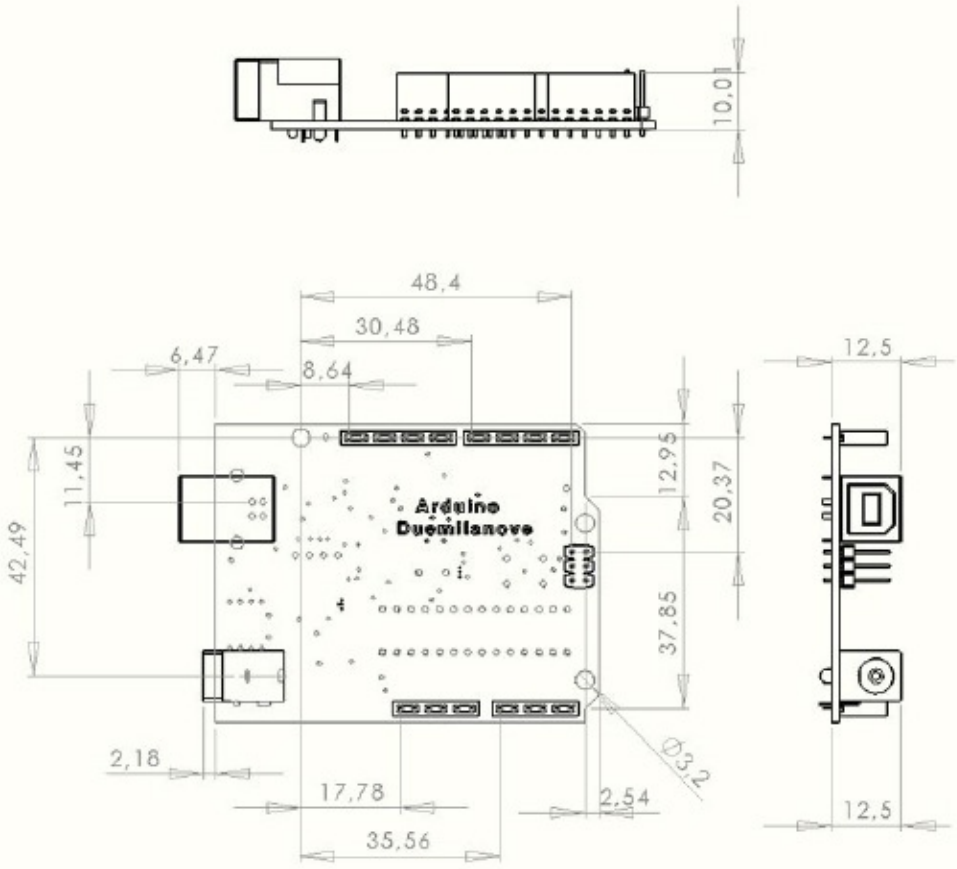

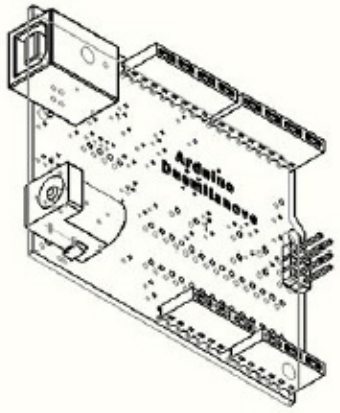

Appendix B: Specification Sheets

Motor Specification Sheet

206-109

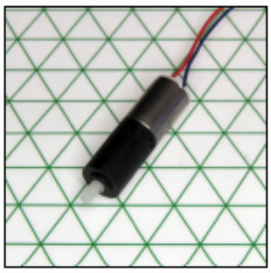

6mm DC Gearmotor - 19mm Type
Shown on 6mm Isometric Grid

PRECISION MICRODRIVES™

Product Data Sheet
Nano Planetary™
6mm DC Gearmotor - 19mm Type

Model: 206-109

Ordering Information

The model number 206-109 fully defines the model, variant and additional features of the product. Please quote this number when ordering.
For stocked types, testing and evaluation samples can be ordered directly through our online store.

Datasheet Versions

It is our intention to provide our customers with the best information available to ensure the successful integration between our products and your application. Therefore, our publications will be updated and enhanced as improvements to the data and product updates are introduced.
To obtain the most up-to-date version of this datasheet, please visit our website at:
www.precisionmicrodrives.com
The version number of this datasheet can be found on the bottom left hand corner of any page of the datasheet and is referenced with an ascending R-number (e.g. R002 is newer than R001). Please contact us if you require a copy of the engineering change notice between revisions.

If you have any questions, suggestions or comments regarding this publication or need technical assistance, please contact us via email at:
enquiries@precisionmicrodrives.com or call us on +44 (0) 1932 252 482

Key Features

Body Diameter:	6 mm [+/- 0.1]
Body Length:	18.7 mm [+/- 0.2]
Shaft Orientation:	Inline
Gear Ratio:	136 :1
Gearhead Type:	Planetary
Rated Operating Voltage:	3 V
Rated Torque:	3 mNm
Rated Speed:	140 rpm
Typical Max. Output Power:	75 mW

Typical DC Gearmotor Performance Characteristics

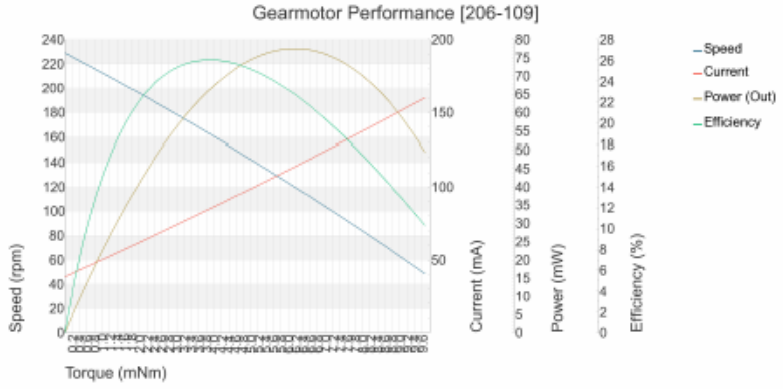

Physical Specification

PARAMETER	CONDITIONS	SPECIFICATION
Body Diameter	Max body diameter or max face dimension where non-circular	6 mm [+/- 0.1]
Body Length	Excl. shafts, leads and terminals	18.7 mm [+/- 0.2]
Unit Weight		1.2 g
No. of Output Shafts		1
Shaft Diameter		2 mm
Shaft Orientation		Inline
Shaft Length	Measured from motor body face	3.6 mm [+/- 0.2]

Construction Specification

PARAMETER	CONDITIONS	SPECIFICATION
Gear Ratio		136 :1
Gearhead Type		Planetary
Motor Construction		Coreless
Commutation		Precious Metal Brush
Rotation Direction	As viewed from the primary shaft end / or motor top	CW
No. of Poles		3
Bearing Type		Sintered Bronze

Leads & Connectors Specification

PARAMETER	CONDITIONS	SPECIFICATION
Lead Length	Lead lengths defined as total length or between motor and connector	100 mm [+/- 5]
Lead Strip Length		1.5 mm [+/- 0.5]
Lead Wire Gauge		32 AWG
Lead Configuration		Straight

Operational Specification

PARAMETER	CONDITIONS	SPECIFICATION
Rated Operating Voltage		3 V
Rated Torque		3 mNm
Rated Speed	At rated voltage under fixed torque at rated load	140 rpm
N/L Speed	Measured at rated voltage	240 rpm [+/- 35]
Max. N/L Current	Measured at rated voltage	45 mA
Max. Start Voltage	Measured at no load	0.5 V
Max. Operating Voltage		3.6 V
Max. Start Current	At rated voltage	230 mA
Max. Rated Current	At rated voltage under fixed torque at rated load	90 mA
Min. Insulation Resistance	At 50V DC between motor terminal and case	1 MOhm

Arduino Specification Sheet

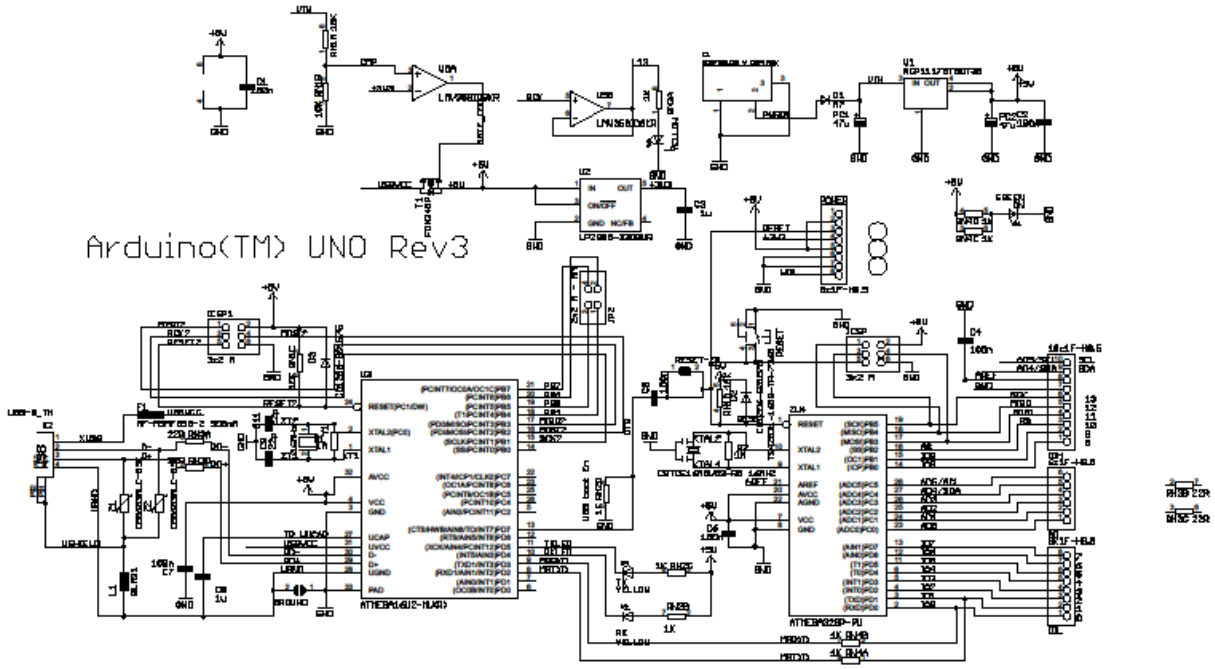

Arduino UNO

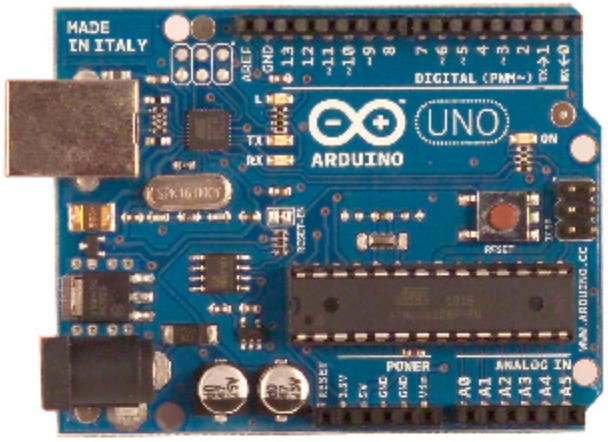

CE

Product Overview

The Arduino Uno is a microcontroller board based on the ATmega328 (datasheet). It has 14 digital input/output pins (of which 6 can be used as PWM outputs), 6 analog inputs, a 16 MHz crystal oscillator, a USB connection, a power jack, an ICSP header, and a reset button. It contains everything needed to support the microcontroller; simply connect it to a computer with a USB cable or power it with a AC-to-DC adapter or battery to get started. The Uno differs from all preceding boards in that it does not use the FTDI USB-to-serial driver chip. Instead, it features the Atmega8U2 programmed as a USB-to-serial converter.

"Uno" means one in Italian and is named to mark the upcoming release of Arduino 1.0. The Uno and version 1.0 will be the reference versions of Arduno, moving forward. The Uno is the latest in a series of USB Arduino boards, and the reference model for the Arduino platform; for a comparison with previous versions, see the index of Arduino boards.

Index

Technical Specification

EAGLE files: arduino-duemilanove-uno-design.zip Schematic: arduino-uno-schematic.pdf

Summary

Microcontroller	ATmega328
Operating Voltage	5V
Input Voltage (recommended)	7-12V
Input Voltage (limits)	6-20V
Digital I/O Pins	14 (of which 6 provide PWM output)
Analog Input Pins	6
DC Current per I/O Pin	40 mA
DC Current for 3.3V Pin	50 mA
Flash Memory	32 KB of which 0.5 KB used by bootloader
SRAM	2 KB
EEPROM	1 KB
Clock Speed	16 MHz

the board